

## Technical memorandum

---

|                 |   |
|-----------------|---|
| From            | Matt Wickham, Principal Advisor, Geochemistry, Growth and Innovation  |
| Department      | Growth & Innovation   |
| To              | Victoria Peacey, Senior Manager – Permitting and Approvals, Resolution Copper                                     |
| CC              | Ted Eary (Enchemica), Mark Logsdon (Geochimica), Kate Duke (Duke HydroChem), Tim Bayley (Montgomery & Associates) |
| Reference       | Prediction of tailings seepage water chemistry influenced by tailings weathering processes                        |
| Date            | 23 August 2018 (Final)  |
| Number of pages | 30  |

### 1.0 Introduction

The draft environmental impact statement (DEIS) for the Resolution Copper mine includes assessment of the following tailings storage facility alternatives:

- Alternative 1: No Action
- Alternative 2: Near West Modified Proposed Action – “Wet”
- Alternative 3: Near West Modified Proposed Action – “Dry”
- Alternative 4: Silver King Filtered
- Alternative 5: Peg Leg
- Alternative 6: Skunk Camp

The process circuit and post-closure seepage chemistries for these alternatives could be affected by weathering processes within the tailings following placement. The geochemically dominant processes are sulfide oxidation and subsequent gangue mineral dissolution, with attendant solute release to tailings porewater. Predictions of the chemical compositions of tailings porewater and seepage during the mine’s operation and after closure is the focus of this document. The specific objectives of the tailings porewater predictions are:

- Predict porewater chemistry within the final scavenger embankment profile and beach areas for alternatives 2, 3, 5, and 6 during operations and post closure;
- Predict porewater chemistry for the entire filtered scavenger tailings for alternative 4 during operations and post closure;
- Predict a mixed seepage chemistry and solute load for represented areas during operations for comparison to the process circuit chemistry predictions; and
- Predict a mixed seepage chemistry and solute load for the represented areas for use in post closure water management planning.

## 1.2 Scope

The conditions represented by the predictions include those areas of the storage facilities with the greatest potential for substantial oxygen ingress and porewater drainage. For alternatives 2, 3, 5, and 6, the area of interest is the embankments and near beach areas. The embankments will be constructed of cyclone sands, and will be well-drained, thereby allowing some amount of oxygen ingress and vertical transport of reaction products. The near-beach areas are also expected to include some coarser materials resulting from particle size segregation during spigotting. By comparison, the interior areas will be composed of fine-grained scavenger tailings, including the pyrite tailings, which are expected to exhibit a low vertical permeability and high moisture content. The pyrite tailings will be managed subaqueously during operations and then buried by a thick sequence of fine-grained scavenger tailings and a store and release cover to reduce oxygen ingress and infiltration. Under these conditions, oxygen will not penetrate into the tailings at rates sufficient<sup>1</sup> to affect seepage chemistry for hundreds of years, and as such, these areas are not included in the predictions. For Alternative 4, oxygen is likely to penetrate the entire surface area of the whole scavenger tailings (and the pyrite tailings) during deposition and into post closure. The area of interest for Alternative 4, therefore, is the entire scavenger tailings facility surface. Contact water chemistry for the pyrite tailings for Alternative 4 is described by Enchemica (2018c) and is considered to be also indicative of seepage water.

All predictions were completed for the 41 years of operation and an additional 204 years post closure, or 245 years total. The model approach, assumptions, inputs, and results are described in the following sections.

## 2.0 Model approach

The SOX-MIM (**S**ulfide **O**Xidation **M**obile-**I**Mmobile model (Ver 1.8)) developed by Rio Tinto Growth & Innovation and Dr. L. E. Eary (Enchemica LLC) was used for this application. The model includes two modules: a one-dimensional profile module and a mixing module. The profile module predicts porewater chemistry over time within a vertical tailings profile. The mixing module processes the profile module results to generate a single “mixed” seepage chemistry for a TSF when supplied with a facility construction schedule and design that includes timing of tailings deposition and embankment construction, tailings thickness, and exposed area.

The SOX-MIM model employs PHREEQC version 3 (Parkhurst and Appelo 2013, release 3.4.0) for reactive processes that affect water chemistry, including aqueous speciation, solubility, redox, adsorption, and physical non-equilibrium (mobile-immobile) transport of both water and solutes.

The O<sub>2</sub> ingress rate for the profile module is calculated as a function of the oxygen diffusion rate through the surface of unsaturated tailings and simultaneous consumption by sulfide mineral oxidation (Elberling et al. 1994; Elberling and Nicholson, 1996). The rate and extent of sulfide mineral oxidation in unsaturated tailings are primarily a function of the rate of oxygen ingress by diffusion through the air-filled pore space. Only a very minor portion of O<sub>2</sub> is transported in the aqueous phase. The numerical model approach used by the SOX-MIM profile module is based on a simple conceptual model of the oxidation of pyrite in porous media in which the oxidation proceeds through the tailings in a series of steps. The model is based on the concept of a constant intrinsic oxidation rate (IOR) of a reactive material. The mathematical approach is based on Davis and Ritchie (1986, 1987) as implemented by Gibson et al. (1994).

Assuming the tailings profile is homogeneous, with an oxygen diffusion coefficient  $D$ , oxygen will initially penetrate a distance  $x_1$ , given by:

---

<sup>1</sup> KCB (2016) conducted unsaturated flow modeling for the scavenger fines and pyrite tailings under atmospheric (\*post-closure) conditions. The simulations predicted that while the net infiltration for covered fine and pyrite tailings is low, the low vertical saturated hydraulic conductivity will severely limit the downward moisture redistribution within the profile. For covered conditions, the saturation levels for the fines and scavenger tailings was predicted to remain above 85%,

$$\Delta x_1 = \sqrt{\frac{2DC_o}{S'}} \quad (1)$$

where  $C_o$  is the atmospheric oxygen concentration and  $S'$  is the IOR.

In accordance with the constant IOR model, this zone will oxidize uniformly throughout this diffusion length until all sulfides are oxidized. Thereafter, the zone becomes inert and the oxygen diffuses through the zone to form a new oxidation zone below. The time taken for the oxygen to attain the initial and the next pseudo-steady state is short compared with the time taken to oxidize a zone, and the transition time is ignored in this model. The thickness of subsequent steps progressively reduces due to the increasing thickness of the now unreactive material above. The expression for the thickness of the  $n$ th zone is given as:

$$\Delta x_n = \sqrt{\frac{2DC_o}{S'}} [\sqrt{n} - \sqrt{n-1}] \quad (2)$$

The time,  $t_s$ , for the pyrite in a zone to oxidize fully is given by the ratio of the density of sulfide,  $\rho_{rs}$ , to the IOR, with a stoichiometric factor  $\varepsilon$ , which relates the consumption of sulfide to the consumption of oxygen. The time for each step to oxidize is the same for all steps and is given by:

$$t_s = \frac{\varepsilon \rho_{rs}}{S'} \quad (3)$$

For illustrative purposes, an example of the progression of the oxidation depth is shown on Figure 1. The figure shows the predicted advance of the oxidation depth based on Gibson et al. 1994. for a sulfide content of 0.12 wt %, an IOR of  $2.7 \times 10^{-9}$  kg(O<sub>2</sub>)/m<sup>3</sup>/s, and an oxygen diffusion coefficient ( $D$ ) of  $3.8 \times 10^{-6}$  m<sup>2</sup>/s. Each step, or  $t_s$ , is approximately 47 years for this example, and the total simulation shown is approximately 560 years. For comparison, the predicted reaction front using the numerical model PYROX (Wunderly et al. 1999<sup>2</sup>) is shown, which closely follows the advance of the oxygen diffusion depth computed using SOX-MIM.

To be consistent with the process circuit predictions, both the profile and mixing modules use the WATEQ4F.DAT thermodynamic database for the PHREEQC calculations. This database was modified by the addition of basis species and thermodynamic data for Sb, Be, Co, Cr, Mo, Tl, and V. Thermodynamic data for these elements were obtained from the MINTEQ.V4.DAT database. The chemical balance portions of the model include calculations for:

- Ca, Mg, Na, K, Cl, HCO<sub>3</sub>, SO<sub>4</sub>, SiO<sub>2</sub>, F, NO<sub>3</sub>-N, Al, Sb, As, Ba, Be, B, Cd, Cr, Co, Cu, Fe, Pb, Mn, Mo, Ni, Se, Ag, Tl, Zn, and pH.

Key processes represented in the profile module include:

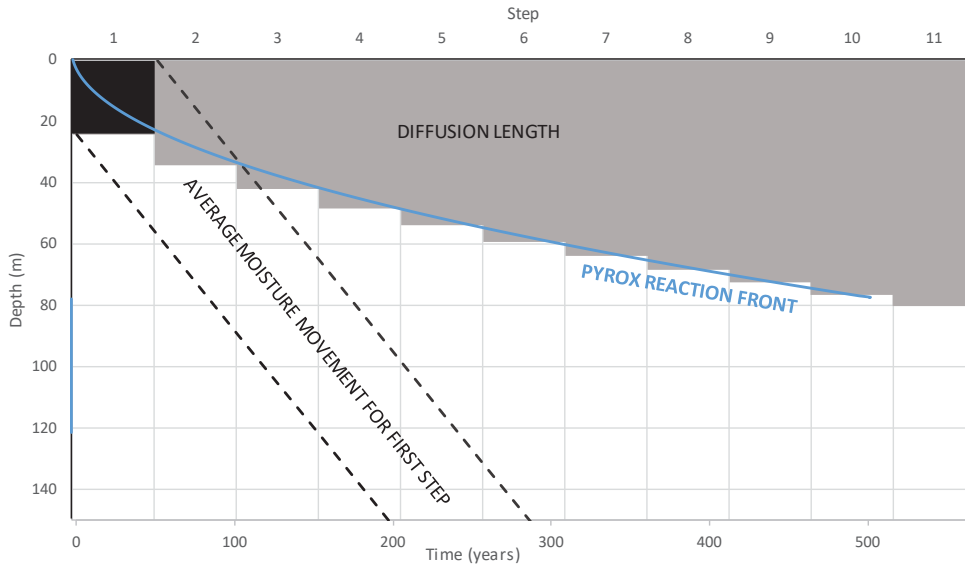
- 1-dimensional (vertical) transport of water and solutes
- kinetic dissolution rates for non-sulfide mineral phases
- modified stoichiometry for solutes (in addition to iron and sulfur) released as a function of sulfide oxidation and silicate weathering
- mineral phase solubility controls on initially calculated solute concentrations
- control of O<sub>2</sub>(g) and CO<sub>2</sub>(g) gas phases
- reversible sorption to selected mineral phases

---

<sup>2</sup> PYROX is a one-dimensional numerical model for kinetic evaluation of movement of oxygen and oxidation of sulfides in tailings. The model accounts for oxygen diffusion from the atmosphere/tailings interface downward through the matrix and across the oxidation rind on the pyrite surface. Pyrite oxidation is represented in PYROX mechanistically and is based on the shrinking core model (Davis and Ritchie, 1986). The model assumes that the oxidation rate is limited by the rate that oxygen is supplied to oxidation sites on the sulfide particles. This rate is dependent on the rate at which oxygen diffuses into the pore space of the tailings and by the rate of diffusion of oxygen into the individual particles of the tailings, through an oxidized shell of secondary oxidation products surrounding an unoxidized core.

- partitioning of the flow and reaction into mobile-immobile domains

Figure 1. Example of the predicted advance of the oxidation depth based on Gibson et al. 1994.



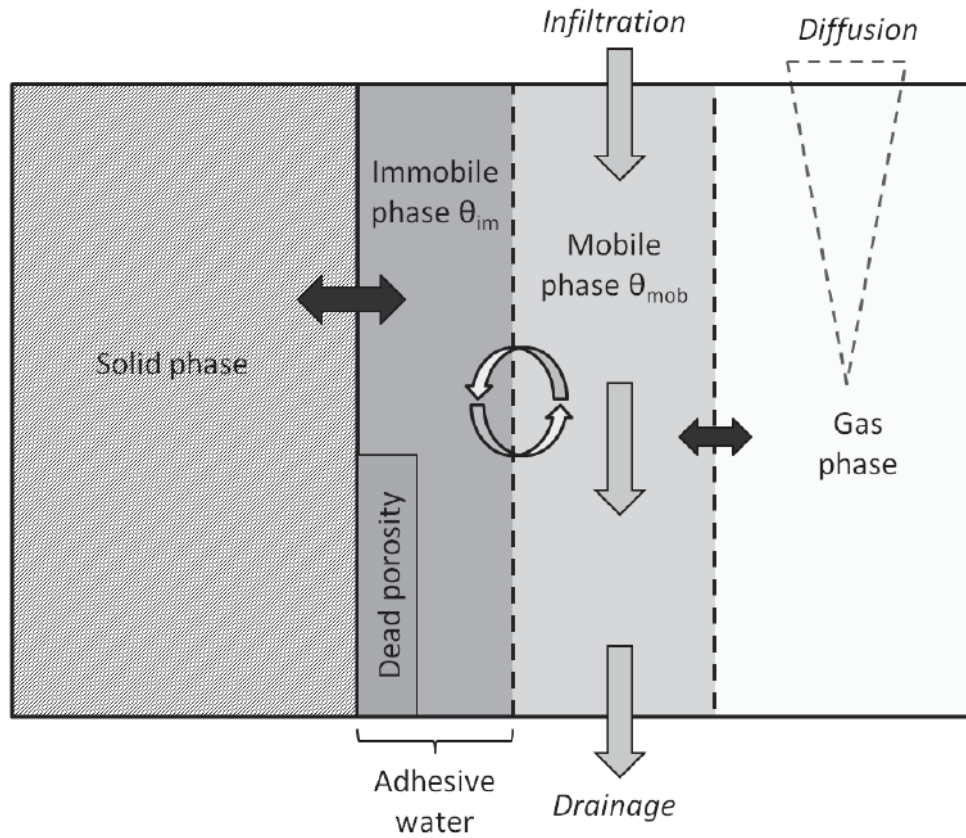
A mobile-immobile conceptual model (MIM) was implemented in the profile module to more accurately describe solute transport behavior in unsaturated, reactive, porous media than could be represented by simulating a bulk flow system (Bond and Wierenga 1990; De Smedt and Wierenga 1984; De Smedt et al. 1986, Gaudet et al. 1977; van Genuchten and Wierenga 1976, Sieland et al. 2016, Jacques et al., 2013, Šimůnek et al. 2009). The conceptual structure of a model cell with physical non-equilibrium (mobile-immobile water) transport (from Sieland et al. 2016) is illustrated on Figure 2. The immobile phase consists of water that entirely wets the solid particle surface and is held by capillary forces. There may be dead water in isolated pores or regions which do not contribute to the contaminant release. The mobile phase is permanently displaced by the input of infiltrating precipitation. The geochemical processes associated with water-tailings interactions, such as pyrite oxidation, mineral dissolution/precipitation, and sorption, and gas phase equilibria, were assumed to take place entirely in the immobile phase. No dead water zones were assumed for the current predictions, and all precipitated mass during the simulation was conservatively allowed to remobilize when conditions permit (e.g. when under-saturated with respect to the mineral phase).

The mobile and the immobile waters are mixed in proportion to their rates of exchange and equilibrated according to the boundary conditions for temperature, gas content, and solubility controls. The mixing proportions in the SOX-MIM as implemented in PHREEQC approach are based on a first order exchange approximation to represent diffusive exchange between mobile and immobile water. The first-order rate expression for diffusive exchange is:

$$\frac{dM_{im}}{dt} = \theta_{im} R_{im} \frac{dC_{im}}{dt} = \alpha (C_m - C_{im}) \quad (4)$$

where subscript  $m$  indicates mobile and  $im$  indicates immobile,  $M_{im}$  are moles of chemical in the immobile zone,  $\theta_{im}$  is porosity of the stagnant (immobile) zone,  $R_{im}$  is retardation in the stagnant zone (unitless),  $C_{im}$  is the concentration in stagnant water (moles per kilogram of water, or mol/kgw),  $t$  is time (s),  $C_m$  is the concentration in mobile water (mol/kgw), and  $\alpha$  is the exchange factor ( $s^{-1}$ ). The retardation is equal to  $R = 1 + dq/dC$ , which is calculated implicitly by PHREEQC through the specified geochemical reactions. The retardation contains the change  $dq$  in concentration of the chemical in the solid due to all chemical processes including exchange, surface complexation, kinetic, and mineral reactions.

Figure 2. Conceptual structure of a model cell with physical non-equilibrium (mobile-immobile water) transport (from Sieland et al. 2016)



The exchange factor  $\alpha$ , as used here, represents both physical and chemical processes such as aqueous diffusion along unsaturated heterogeneous flow paths between the immobile and mobile domains, effects from the formation of secondary mineral phases (e.g. gypsum, metal hydroxides) on the flow system, solute diffusion at reaction surfaces, cementation processes, trapped gasses, and diffusion from dead end pores and pathways. It is not possible to directly measure the exchange factor, but it may be inferred from model calibration to column or field studies.

Solute concentrations in the immobile domain wherein sulfide oxidation is occurring will typically be greater than those in the mobile domain, so mass transfer from the immobile to the mobile domain will occur. Solute diffusion flux from immobile to mobile is described by Fick's Law with a tortuosity factor ( $\xi$ ) to account for the reduced cross-sectional wetted area and longer diffusion pathways:

$$J = -\xi D_o \frac{\partial C}{\partial z} = D_s \frac{\partial C}{\partial z} \tag{5}$$

and

$$\xi = \frac{D_s}{D_o} \tag{6}$$

where

$\xi$  = tortuosity factor

$J$  = solute diffusion flux in a granular material

$D_o$  = solute diffusion coefficient in water

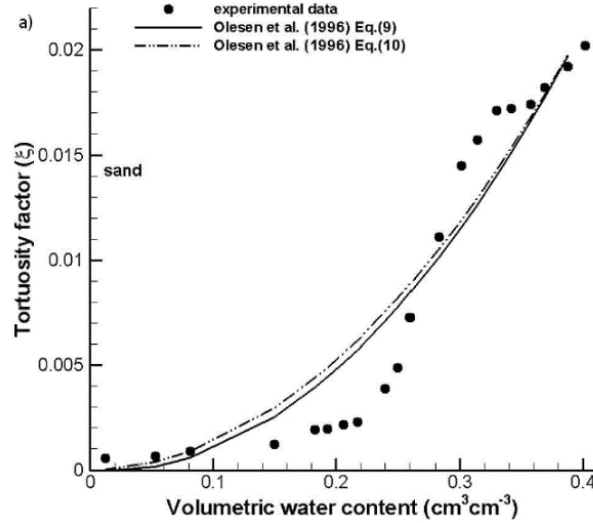
$D_s$  = solute diffusion coefficient in soil

$C$  = solute concentration

$\partial C/\partial z$  = solute concentration gradient along the flux direction  $z$

As shown on Figure 3 (Chou et al. 2012), the tortuosity factor for unsaturated conditions can be low for unsaturated conditions under conservative transport conditions, with the diffusion coefficient in soil ( $D_s$ ) up to 3 orders of magnitude lower than in water ( $D_o$ ). Although the study by Chou et al. (2012) is not explicitly used to guide the selection of the exchange factor for the MIM, it does illustrate the effect on solute diffusion under unsaturated conditions.

Figure 3. Tortuosity factor and volumetric moisture content



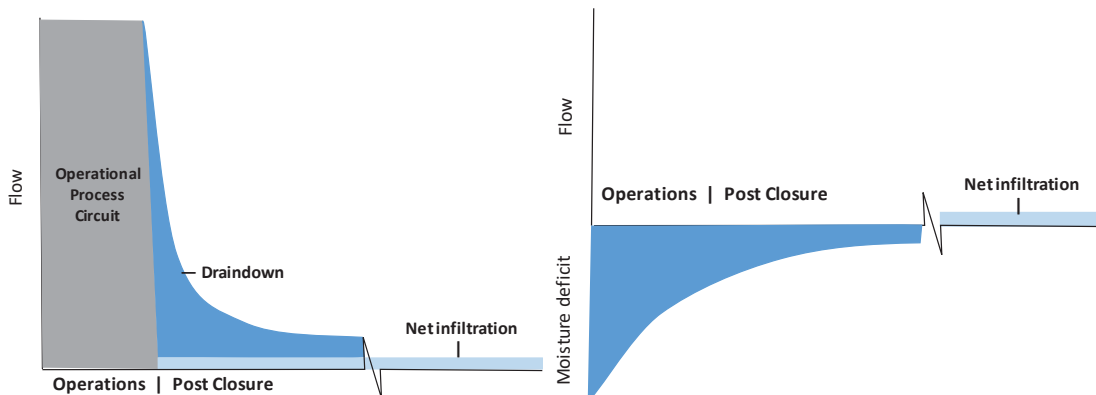
### 3.0 Model inputs

#### 3.1 Hydraulics

A conceptual model for seepage from the tailings impoundment is shown on Figure 4. The hydraulic conditions for most alternatives for which tailings are placed with drainable moisture (Alternatives 2, 3, 5 and 6) can generally be described by three periods:

- Period 1: Operations, during which process water and meteoric precipitation moves through the tailings impoundment to the foundation and seepage collection systems;
- Period 2: Transient post closure, which is initially dominated by gravity drainage of entrained porewater; and
- Period 3: Post closure steady state, when seepage is approximately equal to the net infiltration of meteoric precipitation into the impoundment surface.

Figure 4. Conceptual flow model for tailings seepage (flow) for Alternatives 2, 3, 5, and 6 (left) and Alternative 4 (right)



Estimates of draindown rates and volumes for each alternative are not currently available for all alternatives. Therefore, water chemistry predictions were completed for Period 1 (Enchemica 2018a-f) and for Period 3, as described herein.

Hydraulic inputs are summarized in Table 1 for each of the scenarios. Long-term infiltration rates and the average degree of saturation were based on infiltration modeling for reclaimed conditions (Klohn Crippen Berger [KCB] 2016), with the assumption that infiltration rates for Alternative 4 would be the same as that predicted for slurry tailings. The immobile moisture content was assigned using the estimated residual degree of saturation ( $S_r^{res}$ ), exemplified on Figure 5, from the soil water characteristic curves (SWCCs) from laboratory testing (KCB 2016) for scavenger beach tailings (Alternatives 2, 3, 5, and 6) and for whole scavenger tailings (Alternative 4). It is expected, and assumed for the purposes of these predictions, that the physical and chemical properties of the cyclone sands and near-beach areas would be similar.

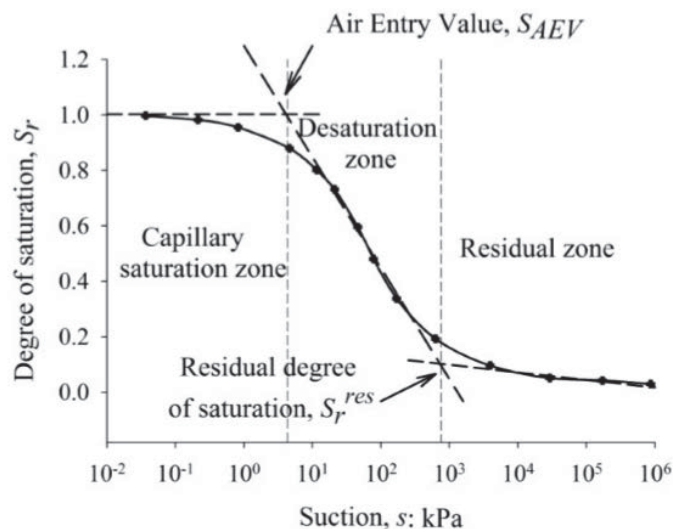
Table 1. Hydraulic inputs

| Alternative                              | Predicted net infiltration rate (inches/year) | Saturation | Moisture Content (vol; immobile) | Moisture Content (vol; mobile) | Mobile porewater velocity (ft/year) |
|--|---|------------|----------------------------------|--------------------------------|-------------------------------------|
| Alt 2                                    | 1.27  | 0.32       | 0.09                             | 0.05                           | 1.2                                 |
| Alt 3                                    | 1.27  | 0.32       | 0.09                             | 0.05                           | 1.2                                 |
| Alt 4: whole scav. tailings as placed    | 0.36  | 0.35       | 0.085                            | 0.07                           | NA                                  |
| Alt 4: whole scav. tailings post closure | 0.36  | 0.545      | 0.17                             | 0.07                           | 0.18                                |
| Alt 5                                    | 1.27  | 0.32       | 0.09                             | 0.05                           | 1.2                                 |
| Alt 6                                    | 1.27  | 0.32       | 0.09                             | 0.05                           | 1.2                                 |

Source: KCB 2016

NA – Not applicable

Figure 5. Typical SWCC showing the regions of desaturation (Vanapalli et al., 1999)



For Alternative 4, whole scavenger tailings are filtered and placed at a moisture content of 35% saturation (15.5% by vol) below long term steady state conditions of 54.5% saturation (24% by vol; KCB 2018d). This moisture deficit is satisfied earlier for thinner portions of the impoundment, and some seepage is predicted during operations. With time, however, all tailings reach a draining moisture content in equilibrium with net infiltration and therefore contribute to seepage.

### 3.2 Tailings surface areas and flows

The scavenger tailings surface areas and thicknesses are summarized for each of the alternatives for selected years in Table 2. Annual values were used in the simulations. All

areas were supplied by the design prepared by KCB (2018a-e) and Golder Associates Inc. (Golder, 2018).

For Alternatives 2, 3, 5, and 6, the areas correspond to the completed embankment surface (sloped and flat) during operations with the addition of the near-beach area at closure. The near-beach areas were estimated to be approximately 1000 feet inward from the embankment crest.

For Alternative 4, the areas included the completed surface for the entire scavenger impoundment. The filtered whole scavenger tailings would be placed at a low moisture content (0.15 by vol), and a lag time was applied to the areas to account for time required to reach field capacity (0.24 by vol) at the estimated recharge rate of 0.36 in/year (KCB 2018d).

Impoundment thicknesses greater than 250 ft were assumed to not generate seepage during the simulation period. All other areas were assumed to linearly increase to the lag time. The estimated lag times and associated areas used in the water chemistry predictions are summarized in Table 3.

*Table 2. Impoundment surface areas represented in the simulations (acres)*

| Thick. (ft)        | 0-50 | 50-100 | 100-150 | 150-200 | 200-250 | 250-300 | 300-350 | 350-400 | >400 | Total |
|--------------------|------|--------|---------|---------|---------|---------|---------|---------|------|-------|
| Alt 2 Area (acres) |      |        |         |         |         |         |         |         |      |       |
| 1                  | 6    | 0      | 0       | 0       | 0       | 0       | 0       | 0       | 0    | 6     |
| 10                 | 60   | 15     | 0       | 0       | 0       | 0       | 0       | 0       | 0    | 75    |
| 20                 | 113  | 72     | 46      | 11      | 0       | 0       | 0       | 0       | 0    | 242   |
| 41                 | 213  | 163    | 151     | 165     | 136     | 96      | 83      | 60      | 29   | 1096  |
| 42                 | 227  | 185    | 186     | 217     | 198     | 143     | 122     | 123     | 94   | 1493  |
| 100                | 227  | 185    | 186     | 217     | 198     | 143     | 122     | 123     | 94   | 1493  |
| 150                | 227  | 185    | 186     | 217     | 198     | 143     | 122     | 123     | 94   | 1493  |
| 200                | 227  | 185    | 186     | 217     | 198     | 143     | 122     | 123     | 94   | 1493  |
| 245                | 227  | 185    | 186     | 217     | 198     | 143     | 122     | 123     | 94   | 1493  |
| Alt 3 Area (acres) |      |        |         |         |         |         |         |         |      |       |
| 1                  | 6    | 4      | 1       | 0       | 0       | 0       | 0       | 0       | 0    | 11    |
| 10                 | 59   | 37     | 16      | 0       | 0       | 0       | 0       | 0       | 0    | 112   |
| 20                 | 104  | 79     | 64      | 50      | 24      | 5       | 0       | 0       | 0    | 326   |
| 41                 | 158  | 124    | 110     | 104     | 106     | 77      | 55      | 44      | 21   | 799   |
| 42                 | 177  | 182    | 150     | 139     | 146     | 138     | 115     | 87      | 88   | 1222  |
| 100                | 177  | 182    | 150     | 139     | 146     | 138     | 115     | 87      | 88   | 1222  |
| 150                | 177  | 182    | 150     | 139     | 146     | 138     | 115     | 87      | 88   | 1222  |
| 200                | 177  | 182    | 150     | 139     | 146     | 138     | 115     | 87      | 88   | 1222  |
| 245                | 177  | 182    | 150     | 139     | 146     | 138     | 115     | 87      | 88   | 1222  |
| Alt 4 Area (acres) |      |        |         |         |         |         |         |         |      |       |
| 1                  | 0    | 0      | 0       | 0       | 0       | 0       | 0       | 0       | 0    | 0     |
| 10                 | 192  | 152    | 11      | 6       | 4       | 0       | 0       | 0       | 0    | 364   |
| 20                 | 192  | 154    | 22      | 12      | 8       | 0       | 0       | 0       | 0    | 388   |
| 41                 | 192  | 166    | 47      | 24      | 18      | 0       | 0       | 0       | 0    | 447   |
| 42                 | 192  | 166    | 48      | 25      | 18      | 0       | 0       | 0       | 0    | 449   |
| 100                | 192  | 166    | 116     | 61      | 44      | 0       | 0       | 0       | 0    | 579   |
| 150                | 192  | 166    | 169     | 91      | 66      | 0       | 0       | 0       | 0    | 684   |
| 200                | 192  | 166    | 169     | 122     | 88      | 0       | 0       | 0       | 0    | 737   |
| 245                | 192  | 166    | 169     | 149     | 108     | 0       | 0       | 0       | 0    | 784   |

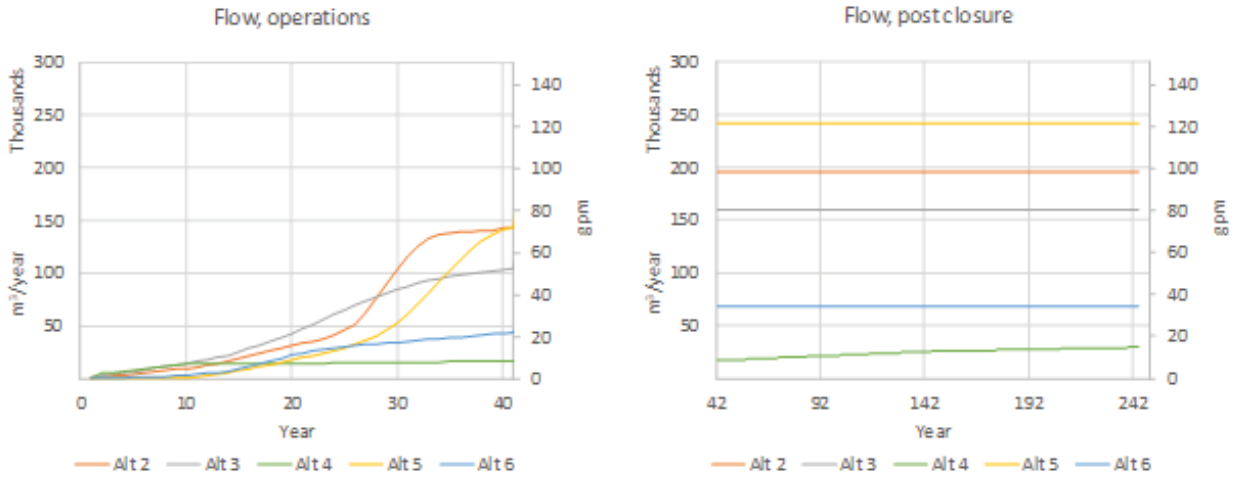
| Thick. (ft)        | 0-50 | 50-100 | 100-150 | 150-200 | 200-250 | 250-300 | 300-350 | 350-400 | >400 | Total |
|--------------------|------|--------|---------|---------|---------|---------|---------|---------|------|-------|
| Alt 5 Area (acres) |      |        |         |         |         |         |         |         |      |       |
| 1                  | 0    | 0      | 0       | 0       | 0       | 0       | 0       | 0       | 0    | 0     |
| 10                 | 1    | 0      | 0       | 0       | 0       | 0       | 0       | 0       | 0    | 1     |
| 20                 | 38   | 51     | 33      | 13      | 0       | 0       | 0       | 0       | 0    | 135   |
| 41                 | 263  | 288    | 251     | 142     | 94      | 54      | 3       | 0       | 0    | 1095  |
| 42                 | 347  | 370    | 333     | 225     | 263     | 302     | 3       | 0       | 0    | 1843  |
| 100                | 347  | 370    | 333     | 225     | 263     | 302     | 3       | 0       | 0    | 1843  |
| 150                | 347  | 370    | 333     | 225     | 263     | 302     | 3       | 0       | 0    | 1843  |
| 200                | 347  | 370    | 333     | 225     | 263     | 302     | 3       | 0       | 0    | 1843  |
| 245                | 347  | 370    | 333     | 225     | 263     | 302     | 3       | 0       | 0    | 1843  |
| Alt 6 Area (acres) |      |        |         |         |         |         |         |         |      |       |
| 1                  | 1    | 0      | 0       | 0       | 0       | 0       | 0       | 0       | 0    | 2     |
| 10                 | 14   | 8      | 4       | 0       | 0       | 0       | 0       | 0       | 0    | 26    |
| 20                 | 35   | 35     | 29      | 26      | 24      | 15      | 6       | 0       | 0    | 170   |
| 41                 | 48   | 55     | 47      | 40      | 41      | 31      | 24      | 24      | 29   | 339   |
| 42                 | 58   | 65     | 59      | 54      | 59      | 44      | 32      | 38      | 111  | 520   |
| 100                | 58   | 65     | 59      | 54      | 59      | 44      | 32      | 38      | 111  | 520   |
| 150                | 58   | 65     | 59      | 54      | 59      | 44      | 32      | 38      | 111  | 520   |
| 200                | 58   | 65     | 59      | 54      | 59      | 44      | 32      | 38      | 111  | 520   |
| 245                | 58   | 65     | 59      | 54      | 59      | 44      | 32      | 38      | 111  | 520   |

Table 3. Seepage lag times and areas for Alternative 4

| Thickness (feet) | Lag time (Years) | Area (acres) |
|------------------|------------------|--------------|
| 0-50             | <41              | 192          |
| 50-100           | <41              | 166          |
| 100-150          | 142              | 169          |
| 150-200          | 284              | 168          |
| 200-250          | 426              | 189          |
| 250-300          | 568              | 156          |
| 300-350          | 710              | 149          |
| 350-400          | 852              | 128          |
| 400-450          | 995              | 109          |
| 450-500          | >1000            | 94           |
| >500             | -                | 283          |

Calculated flows for the operational and post-closure periods are summarized on Figure 6. The increase for Alternatives 2, 3, 5 and 6 between operations and closure is the addition of seepage from the near-beach areas.

Figure 6. Flows



### 3.3 Gas phases and redox

The concentration of O<sub>2</sub> in air (*C<sub>o</sub>*) is primarily a function of temperature and pressure assuming constant percentage by volume of 20.95%. The dry air density was computed using the ideal gas law, expressed as a function of temperature and pressure:

$$\rho = \frac{p}{R_{specific}T} \tag{7}$$

Where:

$\rho$  = air density (kg/m<sup>3</sup>)

*p* = absolute pressure (Pa)

*T* = absolute temperature (K)

*R<sub>specific</sub>* = specific gas constant for dry air (287.058 J/(kg·K))

Absolute pressure is computed for the elevation using the following relationship:

$$p = p_o \left(1 - \frac{Lh}{T_o}\right)^{\frac{gM}{RL}} \tag{8}$$

Where:

*p<sub>o</sub>* = sea level standard atmospheric pressure (101325 Pa)

*T<sub>o</sub>* = sea level standard temperature (288.15 K)

*g* = Earth-surface gravitational acceleration (9.80665 m/s<sup>2</sup>)

*L* = temperature lapse rate (0.0065 K/m)

*R* = universal gas constant (8.31447 J/(mol·K))

*M* = molar mass of dry air (0.0289644 kg/mol)

*h* = height in meters

The atmospheric oxygen concentration was then computed for each site based on the air density and the average annual ambient temperature (21°C).

For partially saturated media, the bulk diffusion constant, *D\**, is equal to the sum of diffusion constants for O<sub>2</sub> in air (*D<sub>a</sub><sup>0</sup>*) and water (*D<sub>w</sub><sup>0</sup>*) (Elberling and Nicholson, 1996):

$$D^* = \tau D_a^0 (1 - S)^\alpha + \tau S D_w^0 / H \tag{9}$$

In Eq. 4, *S* is fractional water saturation by volume,  $\tau$  and  $\alpha$  are fitting parameters equal to 0.273 and 3.28, respectively (Elberling and Nicholson, 1996), and *H* is the dimensionless Henry's Law constant for O<sub>2</sub> (Table 4), which is the ratio of O<sub>2</sub> in air to O<sub>2</sub> solubility in water (= 27.656 at 21°C).

Table 4. Henry's law constants for O<sub>2</sub> with temperature (Langmuir, 1997)

| Temperature (°C) | Henry's Constant |
|------------------|------------------|
| 0                | 0.00218          |
| 5                | 0.00191          |
| 10               | 0.0017           |
| 15               | 0.00152          |
| 20               | 0.00138          |
| 25               | 0.00126          |
| 30               | 0.00116          |
| 35               | 0.00109          |
| 40               | 0.00103          |
| 50               | 0.000932         |

The value of  $D_a^0$  can be calculated as a function of air pressure ( $P_{ap}$ ) and the diffusion temperature effect ( $D_{TE}$ ):

$$D_a^0 = 1.8 \times 10^{-5} \frac{m^2}{s} \left( \frac{100 \text{ kPa}}{P_{ap}} \right) (D_{TE}) \quad (10)$$

Air pressure ( $P_{ap}$ ) is a function of altitude and temperature (Tan et al. 1988). The diffusion temperature effect ( $D_{TE}$ ) is based on the TOUGH method for diffusivity with temperature ( $T_K$ ) in Kelvin (Lefebvre et al. 2001):

$$D_{TE} = \left( \frac{T_K}{273.15 \text{ K}} \right)^{1.8} \quad (11)$$

At 21°C,  $D_a^0 = 2.24 \times 10^{-5}$  m/s.

The value of  $D_w^0$  is a function of temperature and water viscosity and can be calculated from the following equation (Han and Bartells, 1996) in units of cm<sup>2</sup>/s:

$$\log_{10}(D_w^0) \left( \frac{cm^2}{s} \right) = -4.410 + \frac{773.8}{T_K} - \frac{506.4}{T_K^2} \quad (12)$$

The computed diffusion coefficients for oxygen (eq. 9) are  $1.77 \times 10^{-6}$  m<sup>2</sup>/s for Alternatives 2, 3, 5, and 6,  $1.49 \times 10^{-6}$  m<sup>2</sup>/s for Alternative 4 as placed dry, and  $4.64 \times 10^{-7}$  m<sup>2</sup>/s for Alternative 4 long-term post closure.

Gas phases represented in the profile module included O<sub>2</sub>(g) and CO<sub>2</sub>(g). For the porewater chemistry predictions, the partial pressure of oxygen was fixed at atmospheric ( $10^{-0.67}$  atm) at the land surface with a linear percent decrease to zero at the leading edge of the diffusion length computed using Equations 1 and 2. The partial pressure for oxygen below the oxidation front was set to  $10^{-50}$  atm to promote anoxic conditions. The model computed a  $p_e$  below the diffusion front of generally between 0.5 and 2. The partial pressure of CO<sub>2</sub>(g) within the tailings profile was calculated by PHREEQC as a result of reactive processes, with an upper limit set to  $10^{-0.5}$  atm. For the mixing module, the predicted chemistry was equilibrated with atmospheric conditions for both O<sub>2</sub>(g) and CO<sub>2</sub>(g) under the assumption that the seepage would be exposed to atmospheric conditions (surface or shallow vadose zone) or mix with shallow groundwater in equilibrium with atmospheric conditions.

Redox conditions were computed from the O(-2)/O(0) redox couple, which corresponds to the dissolved oxygen/water couple, and the specified dissolved oxygen concentration.

### 3.4 Mineralogy

In 2014, RCM conducted static geochemical testing on 41 samples of scavenger tailings considered to be representative of the scavenger tailings that will be produced by the Resolution mine during operations. Tests included modified Sobek acid-base accounting (ABA), whole rock analysis (WRA) using x-ray fluorescence (XRF) and four-acid digestion with inductively coupled plasma-mass spectrometry (ICP-MS) and net acid generation (NAG) testing with leachate analysis.

Twelve of these scavenger tailings samples were also subjected to humidity cell testing; these samples were submitted for mineralogical characterization by semi-quantitative x-ray diffraction (XRD with Rietveld refinement) and Quantitative Evaluation of Minerals by Scanning Electron Microscopy (QEMSCAN). Detailed results of static and kinetic testing are available from Duke HydroChem (DHC, 2016).

The following sections provide a brief summary of the mineralogy of the scavenger tailings; specifically the amount and type of sulfide, carbonate, and faster-acting silicate minerals represented in the modeling. See DHC (2016) for further details regarding the scavenger tailings mineralogy.

#### 3.4.1 Sulfide Mineralogy

Sulfide sulfur content of the 41 representative scavenger tailings samples ranges between 0.01 and 1.09 weight percent (wt.%) with a median of 0.08 wt.% (DHC, 2016). The geometric mean sulfide sulfur value of 0.07 wt.% was used for all scavenger tailings simulations. The principal sulfide minerals in the scavenger tailings are pyrite and chalcopyrite (on average 51% and 49%, respectively, based on modal analysis using Quantitative Evaluation of Minerals by Scanning Electron Microscopy (QEMSCAN) for scavenger tailings generated from 2014 master ore composites and subjected to humidity cell testing [DHC 2016]). For simplicity, pyrite is used to represent all sulfide minerals in the embankment model. It is recognized that copper-bearing sulfide minerals (e.g., chalcopyrite, chalcocite, and bornite) also contribute to the sulfide-sulfur measured in the scavenger tailings. These phases are not explicitly included in the model; however, the pyrite oxidation rate (POR) and the trace element release rates included in the model are calculated from kinetic test data generated from samples that contain a mixture of iron and copper-bearing sulfides so the resulting kinetic rates represent bulk sulfides.

#### 3.4.2 Carbonate mineralogy

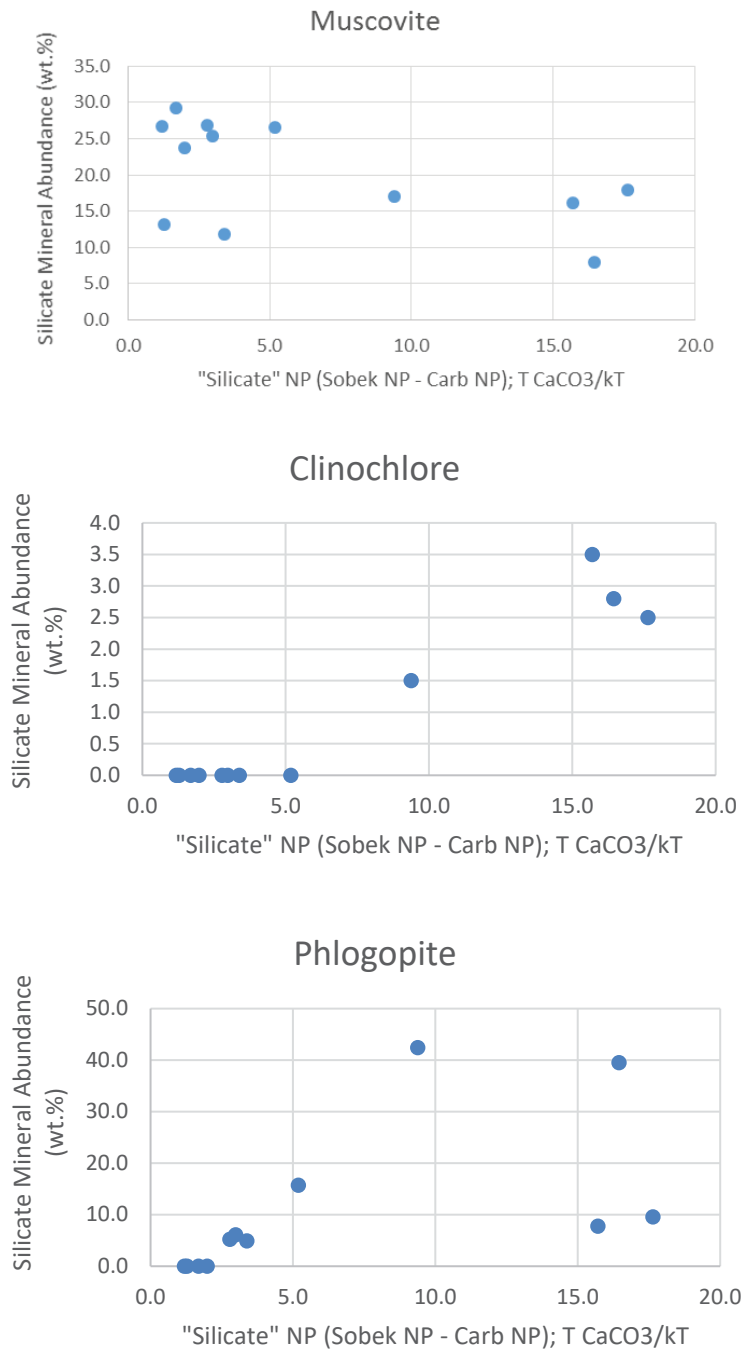
The primary carbonate minerals are calcite and dolomite, making up on average 15% and 61%, respectively, of the carbonate minerals based on modal analysis using QEMSCAN for scavenger tailings generated from 2014 master ore composites and subjected to humidity cell testing (DHC 2016). Carbonate NP in the 41-sample data set ranges between <0.083 and 37.35 T CaCO<sub>3</sub>/kT with a median of 0.25 T CaCO<sub>3</sub>/kT. Carbonate mineralogy is represented in the embankment model by calcite with an assigned abundance equal to the median carbonate NP of 0.25 T CaCO<sub>3</sub>/kT (0.025 wt.% calcite). This is in reasonable agreement with QEMSCAN data from the 12 HCT samples that show a median calcite content of 0.01 wt.% and a median dolomite content of 0.04 wt.% (DHC, 2016). A calcite content of 0.03%, or 0.25 tCaCO<sub>3</sub>/kt, was used for all simulations.

#### 3.4.3 Silicate mineralogy

In addition to the calcium- and magnesium-bearing carbonate minerals, some fast-acting silicate phases can also contribute neutralization potential at rates high enough relative to porewater residence times to neutralize acidity produced during pyrite oxidation. These minerals account for the difference in magnitude between the carbonate neutralization potential and the bulk (modified Sobek) neutralization potential. Figure 7 illustrates the correlation between abundance of muscovite (KAl<sub>3</sub>Si<sub>3</sub>O<sub>10</sub>(OH)<sub>2</sub>), chlorite (clinochlore; Mg<sub>5</sub>Al<sub>2</sub>Si<sub>3</sub>O<sub>10</sub>(OH)<sub>8</sub>), and phlogopite (KAlMg<sub>3</sub>Si<sub>3</sub>O<sub>10</sub>(OH)<sub>2</sub>) vs. silicate NP (Sobek NP – carbonate NP). These plots demonstrate that clinochlore and phlogopite show a positive correlation with silicate NP whereas silicate NP does not appear to be related to muscovite abundance. Based on XRD data, these three silicate minerals (muscovite, clinochlore, and phlogopite) are present in the

Resolution scavenger tailings at median abundances of 20.9, 1.0, and 5.7 wt.%, respectively (DHC, 2016). These values were used for all simulations.

Figure 7. Muscovite, clinochlore, and phlogopite mineral abundances vs. silicate neutralization potential calculated as the difference between bulk (modified Sobek) and carbonate neutralization potential.



### 3.5 Kinetic rate expressions for non-sulfide minerals

Non-sulfide kinetic phases included calcite, muscovite, phlogopite, and chlorite. Kinetic rate expressions for these minerals are summarized in Table 5. The relationship for surface area to mineral volume was based on the bulk particle distribution for the tailings. The expressions incorporated into the model are of the form described by Palandri and Kharaka (2004) and include acid, neutral, and basic mechanisms. The rate parameters are from Palandri and

Kharaka (2004) and Lowsen et al. (2004), with some adjustment to better fit the published experimental data.

Table 5. Mineral dissolution rate parameters

|                       | Acid Mechanism     |                |                | Neutral Mechanism  |                | Carbonate or Basic Mechanism |                |                  |
|-----------------------|--------------------|----------------|----------------|--------------------|----------------|------------------------------|----------------|------------------|
|                       | <sup>a</sup> log k | <sup>b</sup> E | <sup>c</sup> n | <sup>a</sup> log k | <sup>b</sup> E | <sup>a</sup> log k           | <sup>b</sup> E | <sup>c,d</sup> n |
| Calcite               | -0.30              | 14.4           | 1.000          | -5.81              | 23.5           |                              |                |                  |
| Muscovite             | -11.41             | 22             | 0.29           | -15                | 22             | -11.07                       | 22             | 0.27             |
| Phlogopite            |                    |                |                | -12.4              | 29             |                              |                |                  |
| Chlorite <sup>e</sup> | -9.8               | 88             | 0.47           | -13.5              | 88             | -10.7                        | 88             | 0.41             |

a. Rate constant  $k$  computed from  $A$  and  $E$ , 25°C,  $pH = 0$ , mole  $m^{-2} s^{-1}$ .

b. Arrhenius activation energy  $E$ , kJ mole<sup>-1</sup>.

c. Reaction order  $n$  with respect to  $H^+$ .

d. Reaction order  $n$  with respect to  $P(CO_2)$  for calcite

e. Parameters developed based on data from Lowson et al. 2004

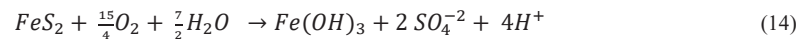
### 3.6 Intrinsic oxidation rates for sulfides

The determination of IOR was based on the form of the rate expression from Williamson and Rimstidt (1994):

$$r \left( \frac{\text{mol py}}{\text{dm}^2 \cdot \text{s}} \right) = k_T \left( \frac{A}{V} \right) \frac{m_{O_2}^{0.5}}{m_{H^+}^{0.11}} \quad \text{where } k_{25C} = 10^{-9.94} \quad (13)$$

The specific rate constant of  $k_{25C} = 10^{-9.94}$  for 25°C was derived from the geometric mean of 10 long-term humidity cell tests (HCTs) conducted with master composite samples of scavenger tailings. The sulfide-S contents in the HCTs averaged 0.15%. The sulfide-S contents and a specific surface area for pyrite of 35 dm<sup>2</sup>/g determined by BET measurements on pyrite tailings were used to calculate  $k_{25C}$ .

The conversion of the HCT kinetic data on SO<sub>4</sub> production into the form of Eq. (13) was based on the following stoichiometry, assuming transformation from ferrous to ferric iron occurs rapidly during the tests:



In converting kinetic data from the HCTs, SO<sub>4</sub> concentrations during the final four weeks of testing were used to calculate oxidation rates. The final four weeks were used because they showed relatively constant pH and leaching rates and were beyond the time needed to rinse out accumulated oxidation products presumably created during sample storage. Also, in converting the SO<sub>4</sub> concentrations to oxidation rates according to Eq. (8), it was assumed there was no limitation of O<sub>2</sub> in the tests, that pH values were not low enough to allow Fe<sup>+3</sup> to be an important oxidant compared to O<sub>2</sub>, and pyrite is the predominant reactive sulfide mineral.

Application of the above parameters yields an IOR value of 1.55 x 10<sup>-9</sup> kg(O<sub>2</sub>)/m<sup>3</sup>/s. This IOR was used to represent the uniform consumption of oxygen according to the model approach described in Section 2.

### 3.7 Solute release

Rates of metal releases were directly linked in the PHREEQC model to the rate of pyrite oxidation, assuming pyrite would be the primary source of most metals released to solution in the embankment. The method for making this linkage was to first determine the molar ratios of metal concentrations to SO<sub>4</sub> concentrations over the last four weeks of HCTs. Geometric means of the molar ratios were then calculated to provide values that could be used as stoichiometric coefficients for pyrite. The geometric means were used because the distributions of release rates were generally found to be lognormal. These calculations result in a modified stoichiometry for pyrite of FeS<sub>2</sub> to  $(Fe_{(1-\Sigma M^{+2})}, M_{i=0 \text{ to } x}^{+2})S_2$ , where M<sup>+2</sup> refers to the various divalent metals that are assumed to be contained in pyrite (e.g., Cd, Co, Cu, Mo, Ni, Pb, Zn). It was also assumed that Ag, As, Ba, Sb, Se, and Tl were released from pyrite in the

same manner as the divalent metals. Elements, such as Ba, are not likely to be present in pyrite, but instead in carbonate minerals. Dissolution of the carbonates is a function of the acidity produced by sulfide oxidation; hence, it was assumed that releases of Ba would be in proportion to sulfide oxidation.

The two exceptions to the approach described immediately above were for B and Si. The rate of Si release was linked to the rates of silicate dissolution (see Section 3.4). The rate of B release was determined from the molar ratios of B to Si in the HCTs and then linked to the silicate dissolution rates. The pyrite and silicate stoichiometry used in the modeling is provided in Table 6.

Table 6. Mineral stoichiometry

| Pyrite     |   |
|------------|---|
| Ag         | 4.17E-07  |
| As         | 3.88E-05  |
| Ba         | 1.36E-03  |
| Cd         | 3.68E-06  |
| Co         | 1.80E-04  |
| Cu         | 1.91E-02  |
| Mn         | 7.23E-03  |
| Mo         | 1.77E-04  |
| Ni         | 3.04E-04  |
| Pb         | 1.85E-06  |
| Sb         | 1.72E-05  |
| Zn         | 1.67E-03  |
| Se         | 1.33E-04  |
| S          | 3.30E-02  |
| FeS2       | 1.00E+00  |
| Silicates  |   |
| Muscovite  | $KAl_3Si_3O_{10}(OH)_2$ 1.0 $H_3BO_3$ 0.0158    |
| Chlorite   | $Mg_5Al_2Si_3O_{10}(OH)_8$ 1.0 $H_3BO_3$ 0.0158 |
| Phlogopite | $KMg_3AlSi_3O_{10}(OH)_2$ 1.0 $H_3BO_3$ 0.0158  |

### 3.8 Solubility controls

Solubility controls were imposed in both the mobile and immobile domains. Predicted porewater chemistry and mixing of seepage will result in solute concentrations that exceed the solubilities of certain secondary mineral phases. It was assumed that some of these minerals will precipitate from solution and will serve as solubility controls for the solutes contained in their structures. Secondary minerals included in the modeling are given in Table 7; phases indicated in bold were found to control concentrations during the simulations. These secondary minerals were selected based on compilations in Eary (1999), Eary and Castendyk (2013), and Nordstrom and Alpers (1999) for the expected pH conditions and low temperatures expected to exist in tailings and within the tailings circuit. Additional metal sulfate salts were included to impose controls, if thermodynamically possible, at high concentrations that might be predicted in the immobile domain.

Table 7. Minerals phases specified as solubility controls

| Mineral phase   | Profile Module, immobile | Profile Module, mobile | Mixing Module |
|---|--------------------------|------------------------|---------------|
| Amorphous Al hydroxide, Al(OH) <sub>3(a)</sub>  | X                        | X                      |               |
| <b>Basaluminite, Al<sub>2</sub>SO<sub>4</sub>·7H<sub>2</sub>O</b>   | <b>X</b>                 | <b>X</b>               | <b>X</b>      |
| Alunite, KAl <sub>3</sub> (SO <sub>4</sub> ) <sub>2</sub> (OH) <sub>6</sub>   | X                        | X                      |               |
| Anglesite, PbSO <sub>4</sub>  | X                        | X                      |               |
| Anhydrite, CaSO <sub>4</sub>  | X                        | X                      |               |
| Antlerite, Cu <sub>3</sub> (OH) <sub>4</sub> SO <sub>4</sub>  | X                        | X                      | X             |
| Atacamite, Cu <sub>2</sub> Cl(OH) <sub>3</sub>  | X                        | X                      |               |
| <b>Barite, BaSO<sub>4</sub></b>   | <b>X</b>                 | <b>X</b>               | <b>X</b>      |
| Bianchite, (Zn,Fe)SO <sub>4</sub> ·6H <sub>2</sub> O  | X                        | X                      |               |
| Brochantite, Cu <sub>4</sub> SO <sub>4</sub> (OH) <sub>6</sub>  | X                        | X                      | X             |
| <b>Calcite, CaCO<sub>3</sub></b>  | <b>X</b>                 | <b>X</b>               | <b>X</b>      |
| Chalcanthite, CuSO <sub>4</sub> ·5H <sub>2</sub> O  | X                        | X                      | X             |
| <b>Chalcedony, SiO<sub>2</sub></b>  | <b>X</b>                 | <b>X</b>               |               |
| Coquimbite, Fe(III) <sub>2</sub> (SO <sub>4</sub> ) <sub>3</sub> ·9(H <sub>2</sub> O)   | X                        | X                      |               |
| Epsomite, MgSO <sub>4</sub> ·7H <sub>2</sub> O  | X                        | X                      |               |
| <b>Ferrihydrite, Fe(OH)<sub>3(a)</sub></b>  | <b>X</b>                 | <b>X</b>               | <b>X</b>      |
| Goslarite, ZnSO <sub>4</sub> ·7H <sub>2</sub> O   | X                        | X                      | X             |
| <b>Gypsum, CaSO<sub>4</sub>·2H<sub>2</sub>O</b>   | <b>X</b>                 | <b>X</b>               | <b>X</b>      |
| Hexahydrite, MgSO <sub>4</sub> ·6(H <sub>2</sub> O)   | X                        | X                      |               |
| Hydromagnesite, Mg <sub>5</sub> (CO <sub>3</sub> ) <sub>4</sub> (OH) <sub>2</sub> ·4H <sub>2</sub> O  | X                        | X                      |               |
| Jarosite(ss), (K <sub>0.77</sub> Na <sub>0.03</sub> H <sub>0.2</sub> )Fe <sub>3</sub> (SO <sub>4</sub> ) <sub>2</sub> (OH) <sub>6</sub>     | X                        | X                      |               |
| Kornelite, Fe(III) <sub>2</sub> (SO <sub>4</sub> ) <sub>3</sub> ·7(H <sub>2</sub> O)  | X                        | X                      |               |
| Langite, Cu <sub>4</sub> (SO <sub>4</sub> )(OH) <sub>6</sub> ·2H <sub>2</sub> O   | X                        | X                      |               |
| Larnakite, Ca <sub>2</sub> SiO <sub>4</sub>   | X                        | X                      |               |
| <b>Malachite, Cu<sub>2</sub>CO<sub>3</sub>(OH)<sub>2</sub></b>  | <b>X</b>                 | <b>X</b>               | <b>X</b>      |
| Melanterite, FeSO <sub>4</sub> ·7H <sub>2</sub> O   | X                        | X                      | X             |
| Mirabilite, Na <sub>2</sub> SO <sub>4</sub> ·10H <sub>2</sub> O   | X                        | X                      |               |
| Morenosite, NiSO <sub>4</sub> ·7(H <sub>2</sub> O)  | X                        | X                      |               |
| Pentahydrite, MgSO <sub>4</sub> ·5(H <sub>2</sub> O)  | X                        | X                      |               |
| Retgersite, NiSO <sub>4</sub> ·6(H <sub>2</sub> O)  | X                        | X                      |               |
| <b>Rhodochrosite(d), MnCO<sub>3</sub></b>   | <b>X</b>                 | <b>X</b>               | <b>X</b>      |
| Rhombochase, H <sub>5</sub> Fe <sup>3+</sup> O <sub>2</sub> ·2(H <sub>2</sub> O) or HFe(SO <sub>4</sub> ) <sub>2</sub> ·4(H <sub>2</sub> O) | X                        | X                      |               |
| Rozenite, Fe <sup>2+</sup> SO <sub>4</sub> ·4(H <sub>2</sub> O)   | X                        | X                      |               |
| Siderite, FeCO <sub>3</sub>   | X                        | X                      | X             |
| SiO <sub>2(a)</sub>   | X                        | X                      | X             |
| Smithsonite, ZnCO <sub>3</sub>  | X                        | X                      | X             |
| Starkeyite, MgSO <sub>4</sub> ·4(H <sub>2</sub> O)  | X                        | X                      |               |
| Thenardite, Na <sub>2</sub> SO <sub>4</sub>   | X                        | X                      |               |

Notes:

(a) denotes amorphous phase

X indicates phase used for simulation

Bold indicates mineral phases that controlled concentration in the PHREEQC calculations

### 3.9 Sorption

Sorption and desorption was simulated only within the mobile phase for the profile module and during mixing by the mixing module. Sorption is expected to occur within the immobile domain, but was conservatively excluded from the simulations due to uncertainties about long-term surface properties for sorbents. The effect of this omission is likely higher predicted concentrations in seepage for some constituents, such as arsenic, cadmium, lead, and copper, than would typically be observed.

Sorption was allowed to occur only to the mass of ferrihydrite precipitated during the simulation. The surface area for ferrihydrite was equal to 600 m<sup>2</sup>/g with a molecular weight of 89 g/mol. Binding sites included the following:

- Hfo\_wOH (weak binding sites) - 0.2 bindings sites (mol/mol Fe)
- Hfo\_sOH (strong binding sites) - 0.005 bindings sites (mol/mol Fe)

### 3.10 Initial porewater chemistry

Initial porewater chemistry was specified for all simulations using median predicted concentrations for operations developed for the process circuit by Enchemica (2018a-f).

An adjustment was made to the initial porewater chemistry for Alternative 4 to account for solute production from sulfide oxidation and silicate weathering while the scavenger tailings remained within the initial calculated oxygen diffusion length. The annual rate of rise for the filtered pile is approximately 25 feet, and the estimated initial oxygen diffusion depth for the as-placed moisture content is 69 ft. This yields an oxidation period of 2.75 years. The solute mass produced during this time period is as described above. The modified porewater chemistry was equilibrated with the solubility controls (immobile domain) and atmospheric conditions, then used as the initial porewater chemistry.

Apart from Alternative 4, the initial porewater chemistry does not account for sulfide oxidation and solute release that might occur during operations and that might report to the process circuit.

#### Active embankment areas

For areas with active embankment construction, tailings will be placed at a high moisture content, but will drain rapidly, thereby allowing oxygen to enter the tailings profile. The depth to which oxygen will diffuse into the tailings depends on the moisture content and the IOR of the tailings. Embankment tailings will be exposed to oxygen until the placement of subsequent tailings (in raises) buries the tailings to a depth below the oxidation front. The duration of the “exposure time” to oxygen is therefore a function of the embankment raise rate for each alternative. Any sulfide release of oxidation product could report rapidly to the process circuit by rinsing from drainage of subsequent tailings raises and by water applied for dust control.

An assessment was undertaken to determine the potential solute load on the process circuit modeling. The approach and results are summarized in Attachment 1. The solute loads were compared to the solute load from the ore moisture and underground sump, which are two of the largest solute loads to the process circuit. The assessment concluded that:

- solute release from sulfide oxidation in the active embankment areas is small compared to other solute loads to the process circuit and likely within the uncertainty of the process circuit chemistry predictions;
- any loads would likely be attenuated, to some degree, by chemical precipitation and sorption processes within the circuit; and
- the process circuit flow and solute balance models prepared by Enchemica do not need to incorporate a source term representing sulfide oxidation in the active embankment areas.

Accordingly, the predicted process circuit chemistry can be used for as initial porewater chemistry without an accounting of solute release from the active embankment areas during operations.

#### Final embankment areas

As an initial assumption, the effect of solute release from sulfide oxidation in the final reclaimed embankment areas will be insignificant during operations and the predicted process circuit chemistry is suitable for initial porewater chemistry. Section 4 of this report compares the predicted chemistry from final embankment areas to the process circuit chemistry to revisit this assumption.

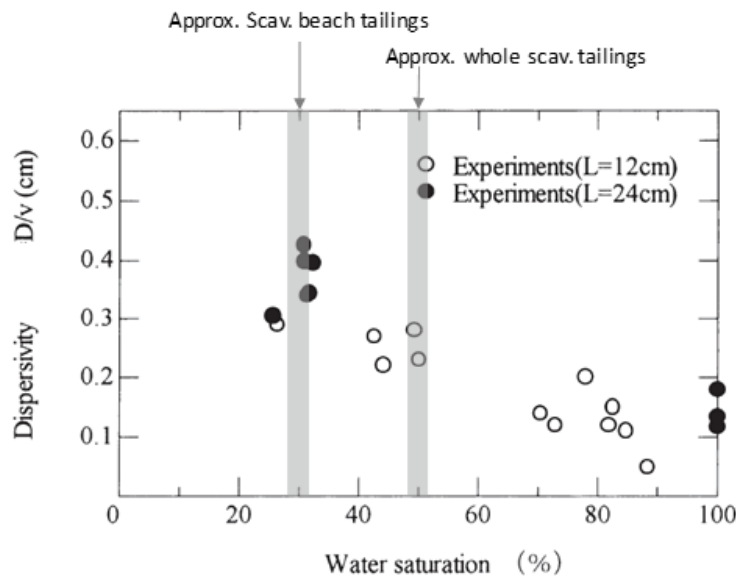
### 3.11 Transport and MIM exchange

Transport of water and solutes in the mobile domain was conducted in PHREEQC using the TRANSPORT keyword, which simulates advection, dispersion, and diffusion. The unsaturated

fluid velocity was constant for the entire simulation and was calculated as the ratio of the annual average net infiltration rate to the average moisture content (Table 1). All transport was simulated at the predicted average moisture content in the mobile tailings domain. The porewater velocity is approximately 1.2 feet per year (ft/year) for Alternatives 2, 3, 5, and 6, or 294 feet in 245 years. The porewater velocity is approximately 0.2 ft/year for Alternative 4, or 44 feet in 245 years. Transport stepping and discretization within PHREEQC was developed so that each shift was 5 calendar years.

Dispersion during transport was represented within the mobile domain. Studies (cited below) have found that at lower water contents a porous medium, including clean sands, has a greater fraction of immobile water, higher dispersion, and slower mass transfer between the mobile and immobile regions. Dispersion was assigned based on the degree of saturation. The dispersivity is generally considered to be an intrinsic property of porous media under fully saturated conditions; however, greater values have been reported for the same media when unsaturated flow conditions are imposed in the system (Padilla et al. 1999, Sato et al. 2000, Maraqa 1997). As granular material desaturates, the number of flow paths decreases, and velocity variations increase, which is manifested as greater dispersion. Sato et al. 1997 reported an increase in the dispersivity by a factor of approximately 2 from saturated conditions to 65% saturation and by a factor of 4.5 to 20% saturation. The cyclone underflow sands and near-beach scavenger tailings were assigned a dispersivity of approximately 0.4 cm, while the filtered whole scavenger tailings were assigned a value of 0.25 cm (Figure 8).

Figure 8. Relation between dispersivity and water saturation (after Sato et al. 2000)



A range of MIM exchange factors,  $\alpha$ , for the simulations was selected by first assessing the sensitivity of the model to a wide range of exchange factors, then selecting a smaller range using guidance from a monitored analogue site. In general, the lower the factor, the greater the ratio of predicted concentrations for the immobile to mobile domains. Exchange increases with higher factors, and the ratio of predicted concentrations approaches the ratio for moisture contents specified for the mobile to immobile domains for the simulated conditions. This is illustrated on Figure 9 for selected constituents for Alternative 2.

The analogue site is the Rio Tinto Kennecott Copper (RTKC) tailings impoundment, for which measured porewater chemistry data are available from suction lysimeters. A summary of the RTKC lysimeter chemistry is provided in Attachment 2. The use of the RTKC lysimeter chemistry to guide selection of the exchange factors is considered conservative, given the much higher sulfide-sulfur content of the RTKC tailings (generally greater than 0.3%) compared to the RCML scavenger tailings (0.07%). Table 8 summarizes the 25<sup>th</sup>, 50<sup>th</sup> (median), and 75<sup>th</sup> quartiles for selected concentrations for the RTKC lysimeters. Data were selected from the lysimeter records within the general pH range predicted for the RCML scavenger tailings. The predicted concentrations using a range of exchange factors (Alternative 2, Table 8) of  $1 \times 10^{-12}$

to  $1 \times 10^{-11} \text{ s}^{-1}$  yield concentrations that are consistent with the range for the 25<sup>th</sup> to 75<sup>th</sup> quartiles. Higher exchange factors yielded porewater concentrations considerably higher than measured for the RTKC lysimeters, and lower exchange factors yielded results that were considered non-conservative (too low). Based on this, a range of exchange factors from  $1 \times 10^{-12}$  to  $1 \times 10^{-11} \text{ s}^{-1}$  was used for all simulations. Results for all simulations are presented in Section 4.

### 4.0 Results

Predicted seepage chemistry is tabulated in Attachment 3 for all alternatives. Time series graphs for selected constituents are provided on Figure 10 and Figure 11 for each of the exchange factors used in the predictions. The results for Alternative 4 in Figures 10 and 11 are specific to the scavenger tailings. Seepage chemistry predictions for the pyrite tailings for Alternative 4 are in Enchemica (2018c).

Predicted concentrations were compared to typical ranges of concentrations for mine and natural waters for a range of geologic conditions and ore types. The reference data are selected constituents by Smith et al. (1994), as presented in Plumlee (1999), which include a subset of the data presented by Plumlee et al. (1999). Those comparisons are shown on Figure 12 for Alternative 2 (which is also indicative of Alternatives 3, 5, and 6) and Figure 13 for Alternative 4. Comparisons for other alternatives (not shown) are similar. There is reasonable agreement between the predicted mobile porewater concentrations and the reference data.

Figure 9. Effect of the exchange factor on predicted concentrations (ratios using concentrations in mg/L), Alternative 2

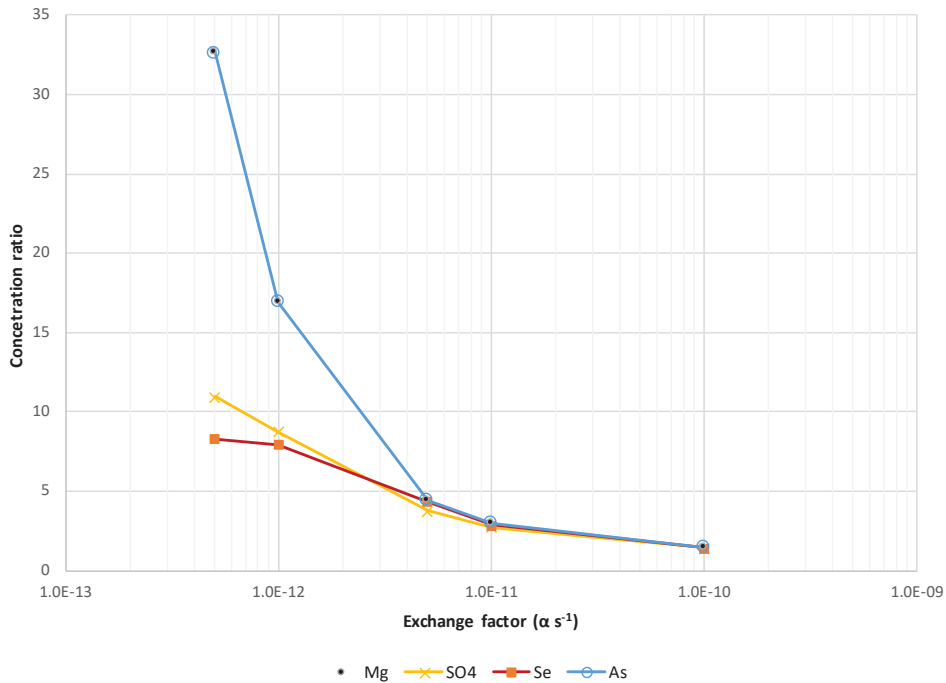


Table 8. RTKC lysimeter chemistry and maximum predicted mobile porewater concentrations, Alternative 2 (shaded areas represent conditions used for RCML scavenger tailings predictions)

| Analyte          | Count | RTKC Lysimeter Chemistry |       |        | Max. predicted porewater concentrations |        |        |        |       |
|------------------|-------|--------------------------|-------|--------|---|--------|--------|--------|-------|
|                  |       | Quartile (%)             |       |        | Mobile, Alternative 2                   |        |        |        |       |
|                  |       | 25                       | 50    | 75     | Exchange Factor (s <sup>-1</sup> )      |        |        |        |       |
|                  |       |                          |       | 1.E-10 | 1.E-11                                  | 5.E-12 | 1.E-12 | 5.E-13 |       |
| * pH (Field)     | 638   | 7.0                      | 7.2   | 7.4    | 7.2                                     | 6.5    | 6.4    | 5.9    | 5.8   |
| Aluminum (mg/L)  | 622   | 0.10                     | 0.27  | 0.60   | 0.73                                    | 0.59   | 0.45   | 0.59   | 0.70  |
| Arsenic (mg/L)   | 641   | 0.0080                   | 0.016 | 0.027  | 0.34                                    | 0.14   | 0.088  | 0.023  | 0.012 |
| Copper (mg/L)    | 649   | 0.020                    | 0.080 | 0.20   | 0.33                                    | 0.20   | 0.20   | 0.20   | 0.20  |
| Fluoride (mg/L)  | 556   | 1.8                      | 2.5   | 3.3    | 2.6                                     | 2.6    | 2.6    | 2.6    | 2.6   |
| Magnesium (mg/L) | 635   | 140                      | 175   | 218    | 4,299                                   | 1,753  | 1,129  | 292    | 152   |
| Manganese (mg/L) | 85    | 0.044                    | 0.19  | 0.72   | 8.4                                     | 2.8    | 1.7    | 1.1    | 1.1   |
| Potassium (mg/L) | 635   | 78                       | 93    | 113    | 1,496                                   | 596    | 385    | 163    | 154   |
| Selenium (mg/L)  | 649   | 0.009                    | 0.018 | 0.040  | 1.37                                    | 0.57   | 0.37   | 0.20   | 0.19  |
| Sulfate (mg/L)   | 585   | 2,180                    | 2,490 | 3,010  | 19,608                                  | 8,633  | 5,989  | 2,552  | 2,048 |
| Zinc (mg/L)      | 635   | 0.050                    | 0.097 | 0.18   | 0.73                                    | 0.59   | 0.45   | 0.59   | 0.70  |

Table 9 summarizes the predicted solute load for the process circuit from ore moisture and the sump (described in Attachment 1). The loads assume average flows during full production and average concentrations for the full life of mine. Table 10 summarizes the solute load for selected constituents from final embankment areas. The loads shown are the *maximum predicted solute* load during the life of mine.

For all constituents, the solute loads from sulfide oxidation in the final embankment areas are about 3% or less of the solute loads from the ore moisture and underground sump. A large amount of lime will be added during processing to maintain circuit pH in the 8 to 8.5 range, therefore, any acidity generated by the precipitation of iron and other metals is unlikely to affect circuit pH.

From this comparison, the following conclusions can be drawn:

- solute release from sulfide oxidation in the final embankment areas during operations is small compared to other solute loads to the process circuit and likely within the uncertainty of the process circuit chemistry predictions;
- any loads would likely be attenuated, to some degree, by chemical precipitation and sorption processes within the circuit;
- the process circuit flow and solute balance models do not need to incorporate a source term representing sulfide oxidation in the final embankment areas; and
- the predicted process circuit chemistry is appropriate for initial porewater chemistry, as used in this modeling.

Figure 10. Time series (by year from start of operations) of predicted seepage concentrations, exchange factor of  $1 \times 10^{-11} \text{ s}^{-1}$

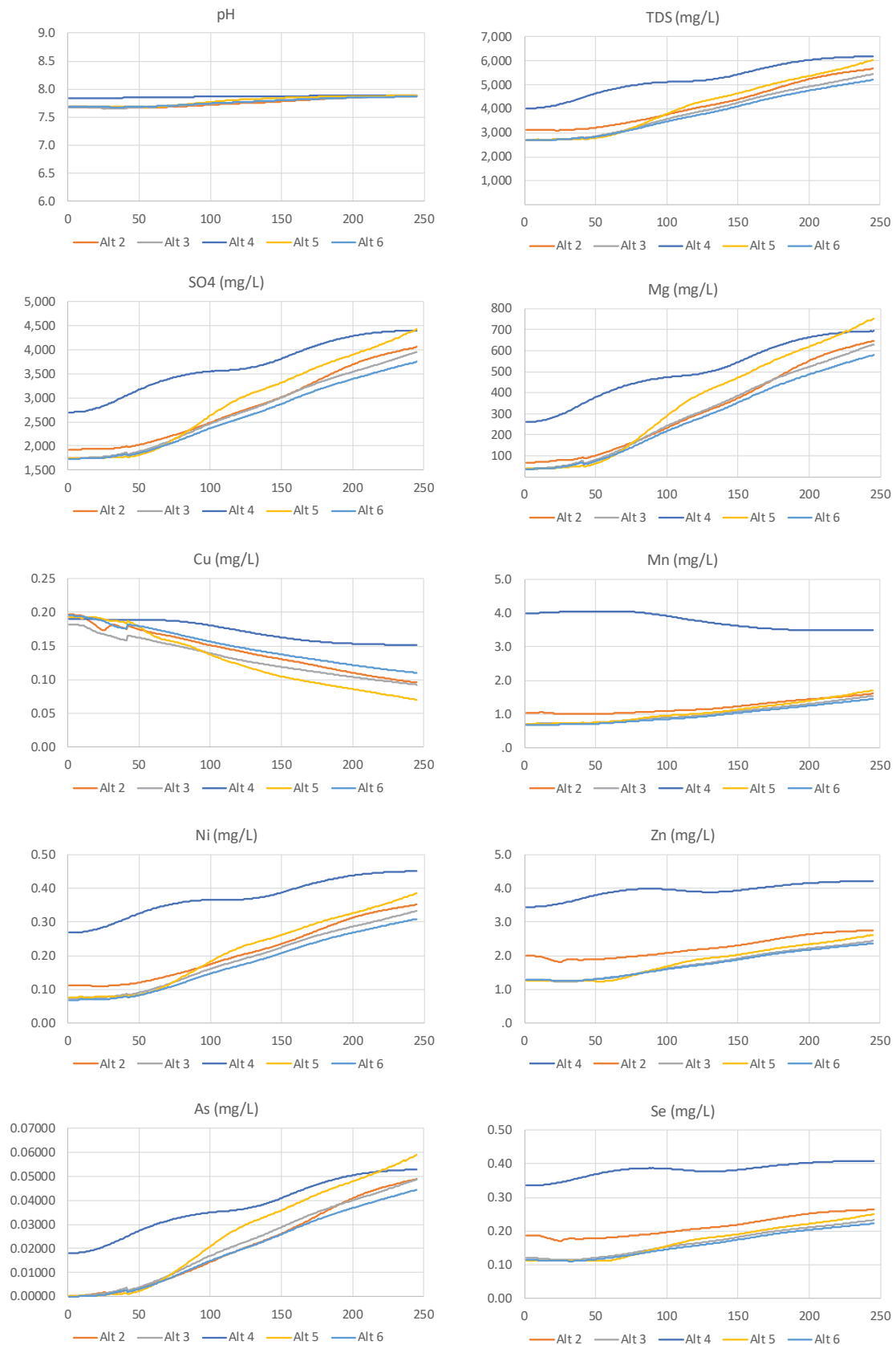


Figure 11. Time series (by year from start of operations) of predicted seepage concentrations, exchange factor of  $1 \times 10^{-12} \text{ s}^{-1}$

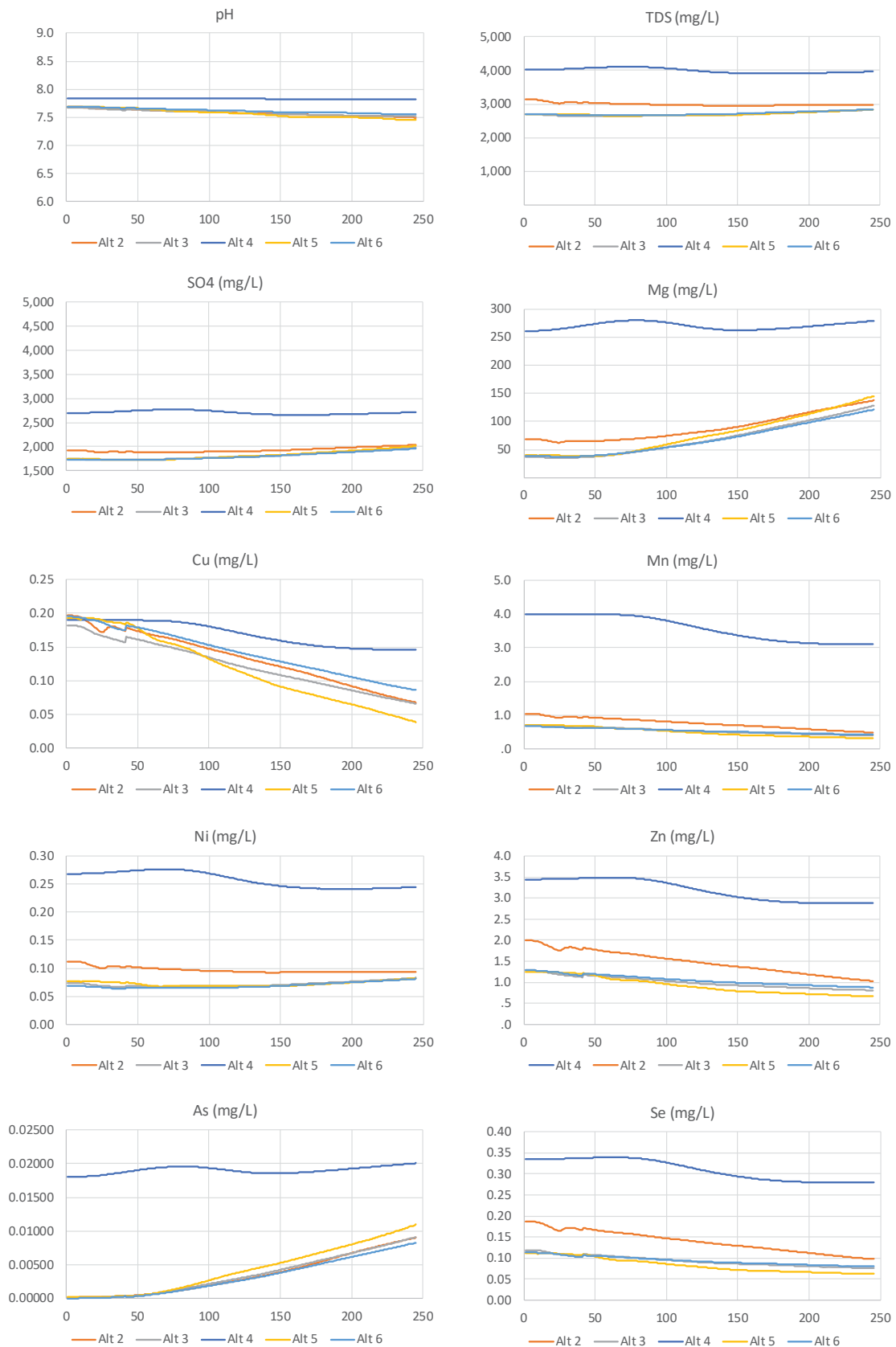


Figure 12. Comparison of predicted mobile porewater concentrations, Alternative 2, reference data from Smith et al. 1994, Plumlee 1999, Plumlee et al. 1999 (predicted values below detection limits not shown; blue and orange markers are predicted concentrations for two MIM exchange factors)

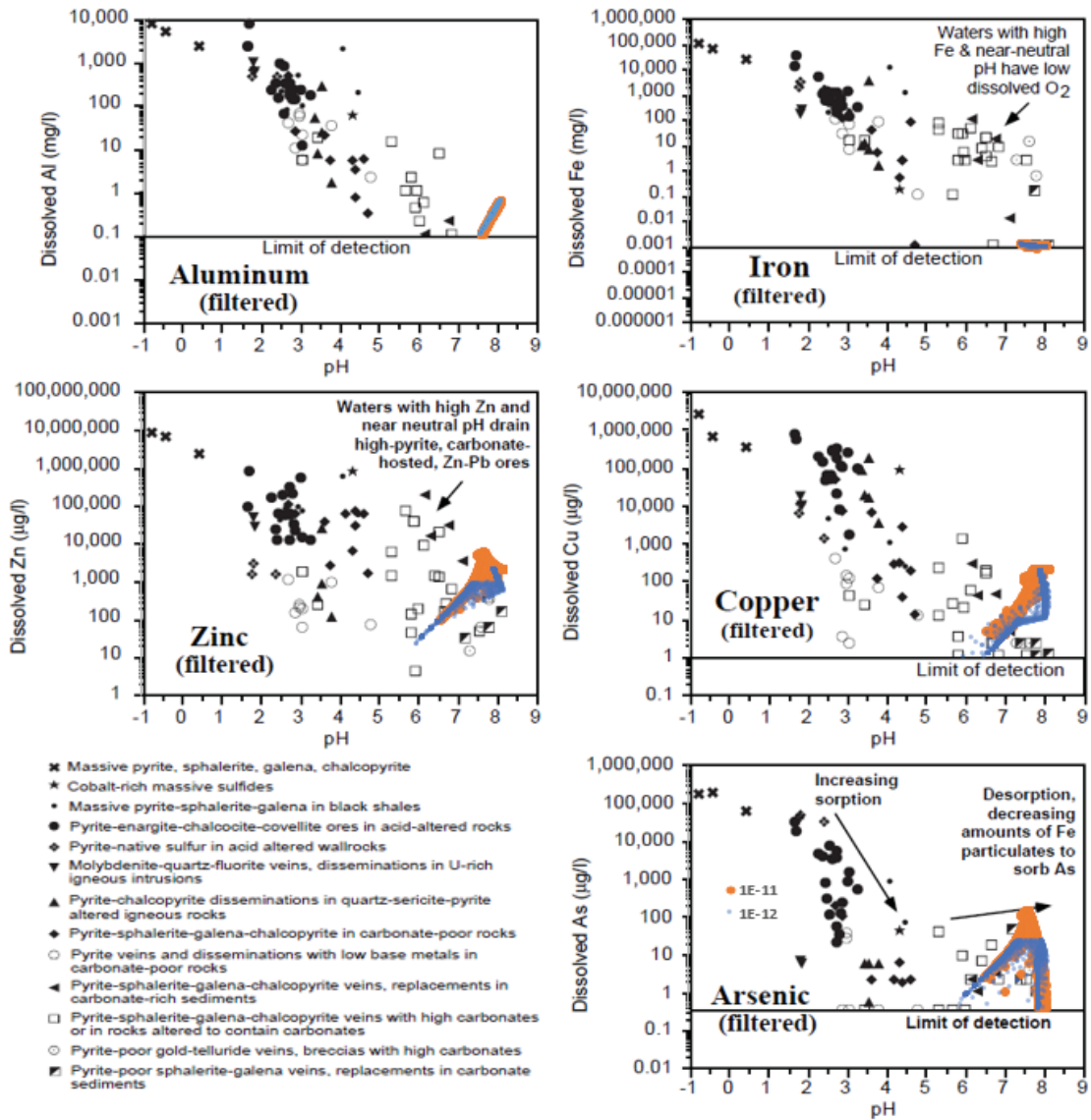
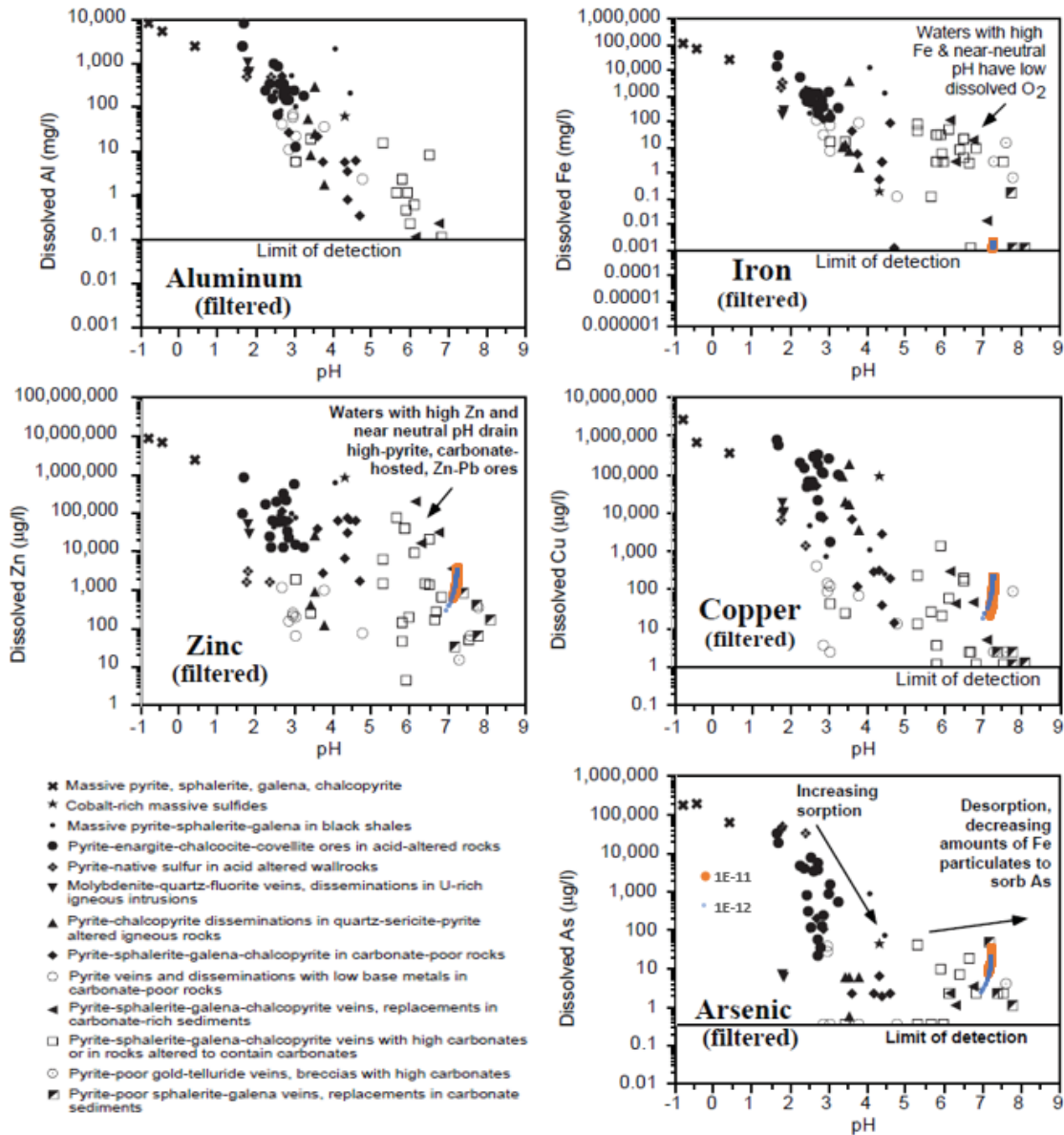


Figure 13. Comparison of predicted mobile porewater concentrations, Alternative 4, reference data from Smith et al. 1994, Plumlee 1999, Plumlee et al. 1999 (predicted values below detection limits not shown; blue and orange markers are predicted concentrations for two MIM exchange factors)



Seepage flows and solute loads are tabulated in Attachment 3. Figure 14 and Figure 15 show time series of predicted solute load for selected constituents.

Figure 14. Time series (by year from start of operations) of predicted solute load, exchange factor of  $1 \times 10^{-11} s^{-1}$

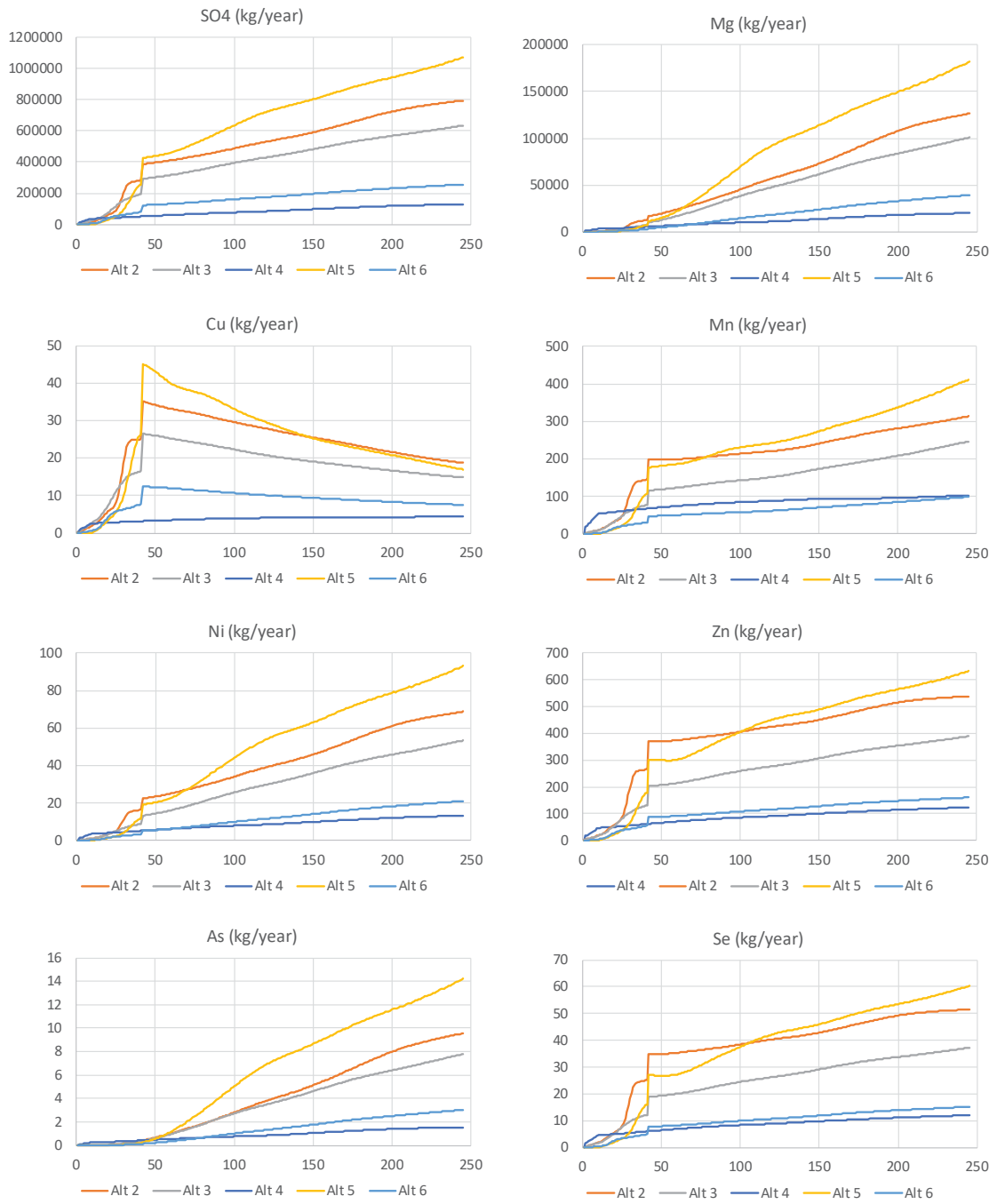


Figure 15. Time series (by year from start of operations) of predicted solute load, exchange factor of  $1 \times 10^{-12} s^{-1}$

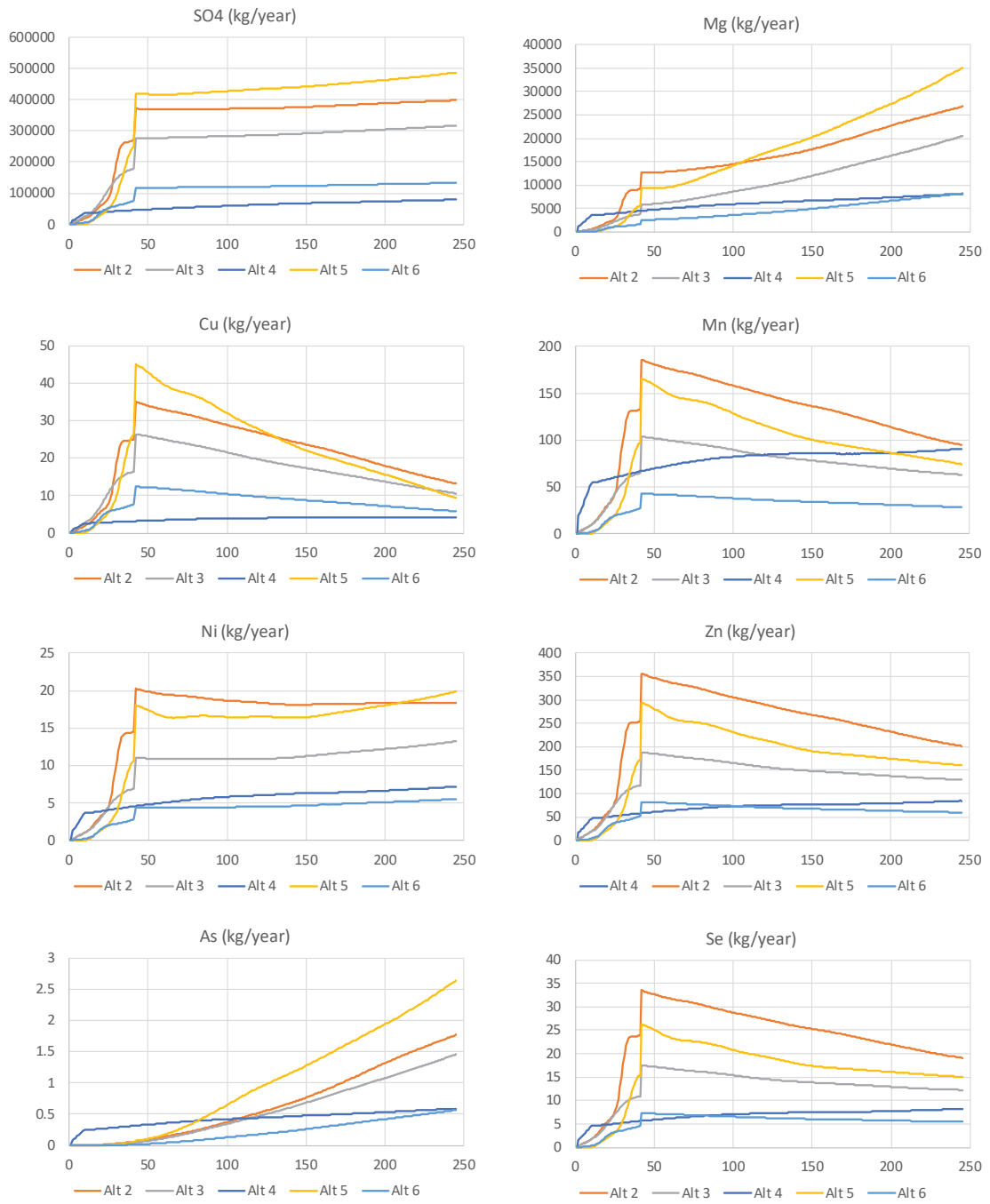


Table 9. Solute load from the ore moisture and underground sump

|                            | Units  | Flow    | Units          | SO4            | Cu             | Fe             | Mn             | Zn             | As             | Se             |
|----------------------------|--------|---------|----------------|----------------|----------------|----------------|----------------|----------------|----------------|----------------|
| <b>Ore Moisture</b>        | gpm    | 914     | mg/L           | 2.8E+03        | 4.6E+02        | 6.3E+01        | 6.0E+00        | 1.3E+01        | 3.5E-02        | 8.5E-01        |
|                            | L/year | 1.8E+09 | mg/year        | 5.1E+12        | 8.3E+11        | 1.1E+11        | 1.1E+10        | 2.3E+10        | 6.4E+07        | 1.5E+09        |
|                            |        |         | kg/year        | 5.1E+06        | 8.3E+05        | 1.1E+05        | 1.1E+04        | 2.3E+04        | 6.4E+01        | 1.5E+03        |
| <b>Sump</b>                | gpm    | 2247    | mg/L           | 9.8E+02        | 1.5E-02        | 2.7E-03        | 2.1E-06        | 2.2E-01        | 6.4E-03        | 4.2E-03        |
|                            | L/year | 4.5E+09 | mg/year        | 4.4E+12        | 6.9E+07        | 1.2E+07        | 9.2E+03        | 1.0E+09        | 2.9E+07        | 1.9E+07        |
|                            |        |         | kg/year        | 4.4E+06        | 6.9E+01        | 1.2E+01        | 9.2E-03        | 1.0E+03        | 2.9E+01        | 1.9E+01        |
| <b>Ore Moisture + Sump</b> |        |         | <b>kg/year</b> | <b>9.5E+06</b> | <b>8.3E+05</b> | <b>1.1E+05</b> | <b>1.1E+04</b> | <b>2.4E+04</b> | <b>9.2E+01</b> | <b>1.6E+03</b> |

Table 10. Maximum predicted solute load from embankment sulfide oxidation during life of mine (denoted SOX)

| <i>Exchange factor = 1 x 10<sup>-11</sup> s<sup>-1</sup></i> | Units   | SO4     | Cu      | Fe      | Mn      | Zn      | As      | Se      |
|--|---------|---------|---------|---------|---------|---------|---------|---------|
| <b>Emb SOX, Alt 2</b>  | kg/year | 2.9E+05 | 2.5E+01 | 1.7E-01 | 1.5E+02 | 2.7E+02 | 3.7E-01 | 2.5E+01 |
| <b>Percent of ore moisture + sump</b>                        | %       | 3.01%   | 0.00%   | 0.00%   | 1.34%   | 1.12%   | 0.41%   | 1.62%   |
| <b>Emb SOX, Alt 3</b>  | kg/year | 1.9E+05 | 1.7E+01 | 1.2E-01 | 7.7E+01 | 1.3E+02 | 3.7E-01 | 1.2E+01 |
| <b>Percent of ore moisture + sump</b>                        | %       | 2.05%   | 0.00%   | 0.00%   | 0.71%   | 0.55%   | 0.40%   | 0.78%   |
| <b>Emb SOX, Alt 5</b>  | kg/year | 2.6E+05 | 2.6E+01 | 1.8E-01 | 1.1E+02 | 1.8E+02 | 2.2E-01 | 1.6E+01 |
| <b>Percent of ore moisture + sump</b>                        | %       | 2.70%   | 0.00%   | 0.00%   | 0.99%   | 0.75%   | 0.23%   | 1.02%   |
| <b>Emb SOX, Alt 6</b>  | kg/year | 8.1E+04 | 7.8E+00 | 5.2E-02 | 3.1E+01 | 5.6E+01 | 1.2E-01 | 5.0E+00 |
| <b>Percent of ore moisture + sump</b>                        | %       | 0.86%   | 0.00%   | 0.00%   | 0.29%   | 0.23%   | 0.13%   | 0.32%   |

Notes: Alternative 4 results not included because seepage from the filter pile is not expected to be significant during life of mine.

## 5.0 References

- Bond, W. J., and P. J. Wierenga 1990 Immobile water during solute transport in unsaturated sand columns, *Water Resour. Res.*, 26, 2475–2481.
- Chou, H., L. Wu, L. Zeng, and A. Chang (2012), Evaluation of solute diffusion tortuosity factor models for variously saturated soils, *Water Resour. Res.*, 48, W10539, doi:10.1029/2011WR011653
- Davis, G. B. and A. I. M. Ritchie. 1986. A model of oxidation in pyritic mine wastes - I. Equations and approximate solutions. *Appl. Math. Model.* 10:314-322.
- Davis, G. B. and A. I. M. Ritchie. 1987. A model of oxidation in pyritic mine wastes - II. Import of particle size distribution. *Appl. Math. Model.* 11:417-422.
- De Smedt, F., and P. J. Wierenga 1984. Solute transfer through columns of glass beads, *Water Resour. Res.*, 20, 225–232.
- De Smedt, F., F. Wauters, and J. Sevilla 1986. Study of tracer movement through unsaturated sand. *Geoderma*. Volume 38, Issues 1–4, September, Pages 223-236
- Duke HydroChem (DHC). 2016. *Geochemical Characterization of Resolution Tailings: Update 2014 - 2016*, Report to Resolution Copper Mining, June 8, 2016.
- Eary, L.E. (1999) Geochemical and equilibrium trends in existing mine pit lakes. *Appl. Geochem.* 14, 963-987.
- Eary, L. E. and D. Castendyk 2013. Hardrock Metal Mining Pit Lakes: Occurrence and Geochemical Characteristics. Chapter 3.2.2 In *Acidic Pit Lakes* (M. Schultz and W. Geller, Eds.), Springer, Berlin, pp. 75-106.

- Elberling, B., R.V. Nicholson, E.J. Reardon, and P. Tibble (1994) Evaluation of sulfide oxidation rates: a laboratory study comparing oxygen fluxes and rates of oxidation product release. *Can. GeoTech. J.*, 31,375-383.
- Elberling, B. and R.V. Nicholson 1996. Field determination of sulfide oxidation rates in mine tailings. *Water Res. Res.* 32, 1773-1784.
- Enchemica 2018a. Alternative 2 - Near West Modified Proposed Action: Prediction of Operational Tailings Circuit Solute Chemistry. Tech. Memo. to V. Peacey (Resolution) from T. Eary (Enchemica), July 17.
- Enchemica 2018b. Alternative 3 - Near West Modified Proposed Action – Thin Lift/PAG Cell: Prediction of Operational Tailings Circuit Solute Chemistry. Tech. Memo. to V. Peacey (Resolution) from T. Eary (Enchemica), July 17.
- Enchemica 2018c. Alternative 4 - Silver King Filtered: Prediction of Operational Tailings Circuit Solute Chemistry. Tech. Memo. to V. Peacey (Resolution) from T. Eary (Enchemica), July 17.
- Enchemica 2018d. Alternative 5 - Peg Leg: Prediction of Operational Tailings Circuit Solute Chemistry. Tech. Memo. to V. Peacey (Resolution) from T. Eary (Enchemica), July 17.
- Enchemica 2018e. Alternative 6 - Skunk Camp Optimized: Prediction of Operational Tailings Circuit Solute Chemistry. Tech. Memo. to V. Peacey (Resolution) from T. Eary (Enchemica), August 14.
- Enchemica 2018f. Common Inputs Common to All Operational Models of Tailings Circuit Solute Chemistry. Tech. Memo. to V. Peacey (Resolution) from T. Eary (Enchemica), July 18.
- Gaudet, J. P., H. Je'gat, G. Vachaud, and P. J. Wierenga 1977. Solute transfer, with exchange between mobile and stagnant water, through unsaturated sand, *Soil Sci. Soc. Am. J.*, 41, 665–671.
- Golder Associates Inc. 2018. EIS Design. Peg Leg Site Alternative 5. Submitted to: Resolution Copper Mining LLC. Document Ref. 1788500-1000-1600-16-R-0. August 6.
- Jacques D, Šimůnek J, Mallants D, van Genuchten MT (2013) The HPx Reactive Transport Models: Summary of Recent Developments and Applications. In: *HYDRUS Software Applications to Subsurface Flow and Contaminant Transport Problems*. Presented at the 4th International HYDRUS Conference, Prague.
- Lefebvre, R., D. Hockley, J. Smolensky, and P. Gélinas 2001. Multiphase transfer processes in waste rock piles producing acid mine drainage 1: conceptual model and system characterization. *J. Contam. Hydr.* 52, 137-164.
- Gibson D.K, G Pantelis and A.I.M Ritchie 1994. The Relevance of the Intrinsic Oxidation Rate to the Evolution of Polluted Drainage from a Pyritic Waste Rock Dump. *Proceedings America Society of Mining and Reclamation*, pp 258-264. Paper presented at the International Land Reclamation and Acid Mine Drainage Conference and the Third International Conference on the Abatement of Acidic Drainage, Pittsburgh, PA, April 24-29.
- Han, P. and D.M. Bartells 1996 Temperature dependence of oxygen diffusion in H<sub>2</sub>O and D<sub>2</sub>O. *J. Phys. Chem.*, 100, 5597-5602.
- Klohn Crippen Berger Ltd. (KCB). 2016. Resolution Copper Project – Near West Tailings Storage Facility Closure Cover Study. Prepared for Resolution Copper Mining. March.
- Klohn Crippen Berger Ltd. (KCB). 2018a. Resolution Copper Project – Tailings Storage Facility DEIS Designs – Tailings Geotechnical Characterization. April.

- Klohn Crippen Berger Ltd. (KCB). 2018b. Resolution Copper Project – DEIS Design for Alternative 3A Near West Modified Proposed Action (Modified Centerline Embankment – “wet”), Rev. 0. June.
- Klohn Crippen Berger Ltd. (KCB). 2018c. Resolution Copper Project – DEIS Design for Alternative 3B Near West Modified Proposed Action (High-density Thickened NPGAG Scavenger and Segregated PAG Pyrite Cell), Rev. 0. June.
- Klohn Crippen Berger Ltd. (KCB). 2018d. Resolution Copper Project – DEIS Design for Alternative 4 Silver King Filtered, Rev. 0. June.
- Klohn Crippen Berger Ltd. (KCB). 2018e. Resolution Copper Project – DEIS Design for Alternative 8 Skunk Camp, Rev. 0. June.
- Lowson, Richard T., M.-C. Josick Comarmond, Geetha Rajaratnam, and Paul L. Brown. 2004. The kinetics of the dissolution of chlorite as a function of pH and at 25°C. *Geochimica et Cosmochimica Acta*, Vol. 69, No. 7, pp. 1687–1699, 2005
- Maraqqa, Munjed A., R.B. Wallace, and T.C. Voice 1997. Effects of degree of water saturation on dispersivity and immobile water in sandy soil columns. *Journal of Contaminant Hydrology* 25, 199-218.
- Nordstrom, D.K. and C.N. Alpers 1999. Geochemistry of acid mine waters. In *The Environmental Geochemistry of Mineral Deposits, Reviews in Economic Geology Vol. 6A* (G.S Plumlee and M.J. Logsdon, Eds.), Soc. Econ. Geol., Littleton, Colorado, p. 133-160.
- Padilla, Ingrid Y., T.-C. Jim Yeh, and Martha H. Conklin 1999. The effect of water content on solute transport in unsaturated porous media. *Water Resources Research*, Vol. 35, No. 11, Pages 3303–3313, November.
- Palandri, J.L. and Kharaka, Y.K. 2004. A Compilation of Rate Parameters of Water-Mineral Interactions Kinetics for Application to Geochemical Modeling. USGS-Report (2004-1068), Menlo Park, California, USA.
- Parkhurst, D.L., and Appelo, C.A.J., 2013, Description of input and examples for PHREEQC version 3—A computer program for speciation, batch-reaction, one-dimensional transport, and inverse geochemical calculations: U.S. Geological Survey Techniques and Methods, book 6, chap. A43, 497 p., available only at <https://pubs.usgs.gov/tm/06/a43/>.
- Plumlee, G.S., Smith, K.S., Montour, M., Ficklin, W.H., and Mosier, E.L., 1999, Geologic controls on the composition of natural waters and mine waters draining diverse mineral-deposit types; in Filipek, L.H., and Plumlee, G.S., (eds.), *The Environmental Geochemistry of Mineral Deposits, Part B. Case Studies and Research Topics: Society of Economic Geologists, Reviews in Economic Geology*, v. 6B, pp.373–432.
- Plumlee, G.S. 1999. The Environmental Geochemistry of Mineral Deposits. In *Reviews Volume 6 Part A: Processes, Techniques, and Health Issues Part B: Case Studies and Research Topics*. (G.S Plumlee and M.J. Logsdon, Eds.), Soc. Econ. Geol., Littleton, Colorado, p. 133-160.
- Sato T., H. Tanahashi H., M. Shibata 2000 Longitudinal Dispersivity of Partially Saturated Sand Packed into Air Suck Column. In: Sato K., Iwasa Y. (eds) *Groundwater Updates*. Springer, Tokyo.
- Sieland, R., T. Metschies, and S. Jahn 2016. Reactive Transport Modelling of the contaminant release from Uranium Tailings using Phreeqc/Excel-coupling *Proceedings IMWA 2016, Freiberg/Germany | Drebenstedt, Carsten, Paul, Michael (eds.), Mining Meets Water – Conflicts and Solutions*.

- Šimůnek, J., K. Huang, and M. Th. van Genuchten, 2009. The HYDRUS Code for Simulating the One-Dimensional Movement of Water, Heat, and Multiple Solutes in Variably-Saturated Media. Research Report No. 144. U.S. Salinity Laboratory, Agricultural Research Service, U.S. Department of Agriculture, Riverside, CA.
- Smith, K.S., Plumlee, G.S., and Ficklin, W.H., 1994, Predicting water contamination from metal mines and mining waste; Notes, Workshop No. 2, International Land Reclamation and Mine Drainage Conference and 3<sup>rd</sup> International Conference on the Abatement of Acidic Drainage: U.S.
- Tan, A., T.X. Zhang, and S.T. Wu (2008) Pressure and density of air in mines. *Indian J. of Radio & Space Physics*, 37, 64-67.
- van Genuchten, M. T., and P. J. Wierenga 1977. Mass transfer studies in sorbing porous media, II, Experimental evaluation with tritium ( $^3\text{H}_2\text{O}$ ), *Soil Sci. Soc. Am. J.*, 41, 272–277.
- Vanapalli, S.K., Fredlund, D.G., and Pufahl, D.E. 1999. The influence of soil structure and stress history on soil-water characteristics of a compacted till. *Geotechnique*, 49(2): 143-159.
- Williamson, M and D. Rimstidt 1994. The kinetics and electrochemical rate-determining step of aqueous pyrite oxidation. *Geochimica et Cosmochimica Acta*. Vol. 58. No. 24, pp. 5443-5454.
- Wunderly, M.D., Blowes, D.W., Frind, E.O. and Ptacek, C.J., 1996. Sulfide mineral oxidation and subsequent reactive transport of oxidation products in mine tailings impoundments: A numerical model. *Water Resources Research*, 32 (10): 3173-3187.

**ATTACHMENT 1**

**Prediction of solute release from tailings weathering processes,  
active embankment construction areas**

## Technical memorandum

---

|                 |   |
|-----------------|---|
| From            | Matt Wickham, Principal Advisor, Geochemistry, Growth and Innovation  |
| Department      | Growth & Innovation   |
| To              | Victoria Peacey, Senior Manager – Permitting and Approvals, Resolution Copper                                     |
| CC              | Ted Eary (Enchemica), Mark Logsdon (Geochimica), Kate Duke (Duke Hydrochem), Tim Bayley (Montgomery & Associates) |
| Reference       | Prediction of solute release from tailings weathering processes, active embankment construction areas             |
| Date            | 23 August 2018 (Final)  |
| Number of pages | 6   |

### 1.0 Introduction

The draft environmental impact statement (DEIS) for the Resolution Copper mine includes assessment of the following tailings storage facility alternatives:

- Alternative 1: No Action
- Alternative 2: Near West Modified Proposed Action – “Wet”
- Alternative 3: Near West Modified Proposed Action – “Dry”
- Alternative 4: Silver King Filtered
- Alternative 5: Peg Leg
- Alternative 6: Skunk Camp

The process circuit for these alternatives could be affected by weathering processes within the tailings during and following placement in the embankment. The geochemically dominant processes are sulfide oxidation and subsequent gangue mineral dissolution, with attendant solute release to tailings porewater. In active embankment construction areas, the solute release will have the potential to rapidly report to the process circuit as newly-placed tailings drain and water is applied for dust control. Predictions of potential solute release from the embankment tailings materials during active placement, and how this might affect the process circuit chemistry, is the focus of this document. The specific objectives of these predictions are:

- Predict solute release from the embankment tailings for alternatives 2, 3, 5, and 6 during active embankment construction and operations;
- Quantitatively compare the solute release rates to selected solute release from other major sources influencing the process circuit; and
- Assess the potential effects on predicted process circuit chemistry.

The conditions represented by the predictions include those areas of the storage facilities with the greatest potential for substantial oxygen ingress and porewater drainage. For alternatives 2, 3, 5, and 6, the area of interest is the embankments. The embankments will be constructed of cyclone sands, and will be well-drained, thereby allowing oxygen ingress and vertical transport of reaction products. By comparison, the interior areas will be composed of fine-grained overflow tailings, including the pyrite tailings, which are expected to exhibit a low vertical permeability and high moisture content. Near beach areas comprised of underflow and whole tailings are expected to be managed wet in order to control dust. The pyrite tailings will be managed subaqueously during operations. Under these conditions, oxygen will not penetrate into the tailings at rates sufficient<sup>1</sup> to affect seepage chemistry for hundreds of years, and as such, these areas are not included in the predictions. For Alternative 4, tailings are placed at a moisture content less than field capacity, and therefore seepage from areas of active deposition is expected to be negligible during operations.

All predictions were completed for the 41 years of operation. The approach, assumptions, inputs, and results for the solute release predictions are described in the following sections.

## 2.0 Approach and inputs

Tailings used to construct the embankments will be placed at a high moisture content, but will drain rapidly, thereby allowing oxygen to enter the tailings profile. The depth to which oxygen will diffuse into the tailings depends on the moisture content and the sulfide intrinsic oxidation rate (IOR) of the tailings. Embankment tailings will be exposed to oxygen until the placement of subsequent tailings (in raises) buries the tailings to a depth below the depth to which oxygen can diffuse. The duration of the “exposure time” to oxygen is therefore a function of the embankment raise rate for each alternative. For the predictions described here, we assume that oxygen penetration to the estimated diffusion depth is instantaneous, that 100% of the solute mass produced by sulfide oxidation is mobilized by drainage from subsequent raises (i.e., no retardation reactions), and that the solutes released from sulfide oxidation report to the process circuit instantly. Dissolution of non-sulfide minerals, such as carbonates and silicates, is not included.

The methodology for computing the oxygen diffusion coefficient, oxygen diffusion depth, and IOR is described in RT G&I (2018). For these predictions, the time required to fully oxidize the sulfides within the diffusion depth greatly exceeds the tailings exposure time. Accordingly, only the initial diffusion depth was considered. The oxygen diffusion coefficient for the tailings was computed assuming an estimated average saturation for the placed tailings of 50% for cyclone sands (about 17% moisture content by volume) in active areas.

The exposure time was estimated for each alternative based on preliminary embankment raise rates provided by Klohn Crippen Berger Ltd. (KCB 2018a,b,c,d) and Golder Associates Inc. (Golder 2018). The rates are summarized in Table 1. Earthen starter dikes were excluded. The pyrite cell embankment for Alternative 4 is relatively small, and was ignored for simplicity. The mass of embankment tailings was provided by KCB and Golder (2018) for the life of mine and was used, with the raise rate, to compute the mass of tailings exposed to oxygen.

Rates of metal releases were directly linked to the rate of pyrite oxidation, assuming pyrite would be the primary source of most metals released to solution in the embankment, as described in RT G&I (2018). The method for making this linkage was to first determine the molar ratios of metal concentrations to  $SO_4$  concentrations over the last four weeks of humidity cell tests (HCTs). Geometric means of the molar ratios were then calculated to provide values that could be used as stoichiometric coefficients for pyrite. The geometric means were used because the distributions of release rates were generally found to be lognormal. These calculations result in a modified stoichiometry for pyrite of  $Fe_{(1-\Sigma M^{+2})}M_{i=0}^{+2}S_2$ ,

---

<sup>1</sup> KCB (2016) conducted unsaturated flow modeling for the scavenger slimes and pyrite tailings under atmospheric (\*post-closure) conditions (KCB 2016). The simulations predicted that while the net infiltration for covered slimes and pyrite tailings is low, the low vertical saturated hydraulic conductivity will severely limit the downward moisture redistribution within the profile. For covered conditions, the saturation levels for the slimes and scavenger tailings was predicted to remain above 85%.

where M<sup>+2</sup> refers to the various divalent metals that are assumed to be contained in pyrite (e.g., Cd, Co, Cu, Mo, Ni, Pb, Zn). It was also assumed that Ag, As, Ba, Sb, Se, and Tl were released from pyrite in the same manner as the divalent metals. The pyrite and silicate stoichiometry used in the modeling is provided in Table 2.

Table 1. Schedules for embankment tailings

| Year | Alternative 2                            |  |                      |                   | Alternative 3                            |  |                      |                   | Alternative 5                            |  |                      |                   | Alternative 6                            |  |                      |                   |
|------|--|--|----------------------|-------------------|--|--|----------------------|-------------------|--|--|----------------------|-------------------|--|--|----------------------|-------------------|
|      | Emb. fill (tons/year x 10 <sup>6</sup> ) | Emb. fill (CY/year x 10 <sup>6</sup> ) | Raise rate (ft/year) | Exp. time (years) | Emb. fill (tons/year x 10 <sup>6</sup> ) | Emb. fill (CY/year x 10 <sup>6</sup> ) | Raise rate (ft/year) | Exp. time (years) | Emb. fill (tons/year x 10 <sup>6</sup> ) | Emb. fill (CY/year x 10 <sup>6</sup> ) | Raise rate (ft/year) | Exp. time (years) | Emb. fill (tons/year x 10 <sup>6</sup> ) | Emb. fill (CY/year x 10 <sup>6</sup> ) | Raise rate (ft/year) | Exp. time (years) |
| 1    | 1.1                                      | 1.7                                    | 0.0                  | 5                 | 1.1                                      | 1.7                                    | 0.0                  | 4                 | 0.0                                      | 0.0                                    | 0.0                  | 3                 | 0.0                                      | 0.0                                    | 56                   | 2                 |
| 2    | 1.5                                      | 2.2                                    | 0.0                  | 4                 | 1.5                                      | 2.2                                    | 0.0                  | 3                 | 0.0                                      | 0.0                                    | 0.0                  | 2                 | 0.0                                      | 0.0                                    | 19                   | 2                 |
| 3    | 2.2                                      | 3.4                                    | 0.0                  | 3                 | 2.2                                      | 3.4                                    | 0.0                  | 2                 | 15                                       | 9.6                                    | 1.0                  | 1                 | 1.7                                      | 2.7                                    | 13                   | 2                 |
| 4    | 4.3                                      | 6.6                                    | 2.9                  | 2                 | 4.3                                      | 6.6                                    | 20                   | 2                 | 1.9                                      | 1.2                                    | 30                   | 1                 | 1.7                                      | 2.7                                    | 18                   | 2                 |
| 5    | 7.1                                      | 11                                     | 14                   | 2                 | 7.1                                      | 11                                     | 20                   | 2                 | 2.0                                      | 1.3                                    | 55                   | 1                 | 1.7                                      | 2.7                                    | 19                   | 2                 |
| 6    | 9.4                                      | 14                                     | 19                   | 2                 | 9.4                                      | 14                                     | 20                   | 2                 | 2.2                                      | 1.4                                    | 39                   | 2                 | 3.3                                      | 5.0                                    | 18                   | 2                 |
| 7    | 11                                       | 17                                     | 20                   | 2                 | 11                                       | 17                                     | 20                   | 2                 | 2.5                                      | 1.6                                    | 20                   | 3                 | 3.3                                      | 5.0                                    | 18                   | 2                 |
| 8    | 12                                       | 19                                     | 21                   | 2                 | 12                                       | 19                                     | 20                   | 2                 | 2.9                                      | 1.9                                    | 16                   | 4                 | 3.3                                      | 5.0                                    | 17                   | 3                 |
| 9    | 12                                       | 18                                     | 20                   | 3                 | 9.4                                      | 14                                     | 18                   | 2                 | 3.4                                      | 2.2                                    | 12                   | 4                 | 3.3                                      | 5.0                                    | 15                   | 3                 |
| 10   | 12                                       | 18                                     | 17                   | 3                 | 9.8                                      | 15                                     | 18                   | 2                 | 4.0                                      | 2.6                                    | 10                   | 5                 | 3.3                                      | 5.0                                    | 14                   | 3                 |
| 11   | 12                                       | 18                                     | 15                   | 3                 | 10                                       | 16                                     | 20                   | 3                 | 4.6                                      | 3.0                                    | 9.0                  | 5                 | 10                                       | 15                                     | 13                   | 3                 |
| 12   | 12                                       | 19                                     | 9.3                  | 3                 | 11                                       | 17                                     | 20                   | 3                 | 5.2                                      | 3.4                                    | 9.0                  | 5                 | 10                                       | 15                                     | 12                   | 3                 |
| 13   | 12                                       | 19                                     | 14                   | 4                 | 11                                       | 17                                     | 12                   | 4                 | 5.7                                      | 3.8                                    | 9.0                  | 5                 | 10                                       | 15                                     | 12                   | 4                 |
| 14   | 13                                       | 20                                     | 15                   | 4                 | 11                                       | 17                                     | 12                   | 4                 | 6.2                                      | 4.0                                    | 8.5                  | 6                 | 10                                       | 15                                     | 12                   | 4                 |
| 15   | 13                                       | 20                                     | 9.0                  | 4                 | 11                                       | 17                                     | 11                   | 4                 | 6.5                                      | 4.3                                    | 8.4                  | 6                 | 10                                       | 15                                     | 11                   | 4                 |
| 16   | 13                                       | 19                                     | 8.5                  | 4                 | 11                                       | 17                                     | 11                   | 4                 | 6.8                                      | 4.4                                    | 8.0                  | 6                 | 9.3                                      | 14                                     | 11                   | 4                 |
| 17   | 13                                       | 19                                     | 9.0                  | 4                 | 11                                       | 16                                     | 11                   | 4                 | 6.9                                      | 4.5                                    | 7.6                  | 7                 | 9.3                                      | 14                                     | 10                   | 4                 |
| 18   | 12                                       | 19                                     | 9.0                  | 4                 | 10                                       | 16                                     | 11                   | 4                 | 7.0                                      | 4.6                                    | 7.2                  | 7                 | 9.3                                      | 14                                     | 9.9                  | 4                 |
| 19   | 12                                       | 19                                     | 9.9                  | 4                 | 9.9                                      | 15                                     | 9.5                  | 4                 | 7.0                                      | 4.5                                    | 6.8                  | 8                 | 9.3                                      | 14                                     | 9.5                  | 4                 |
| 20   | 12                                       | 19                                     | 10                   | 4                 | 10                                       | 15                                     | 9.5                  | 4                 | 6.8                                      | 4.5                                    | 6.5                  | 8                 | 9.3                                      | 14                                     | 9.3                  | 4                 |
| 21   | 13                                       | 19                                     | 10                   | 4                 | 10                                       | 15                                     | 9.5                  | 5                 | 6.7                                      | 4.4                                    | 6.2                  | 8                 | 2.9                                      | 4.4                                    | 9.1                  | 4                 |
| 22   | 13                                       | 19                                     | 10                   | 5                 | 9.9                                      | 15                                     | 9.5                  | 5                 | 6.5                                      | 4.2                                    | 5.9                  | 8                 | 2.9                                      | 4.4                                    | 11                   | 5                 |
| 23   | 13                                       | 19                                     | 8.7                  | 5                 | 8.8                                      | 13                                     | 9.0                  | 4                 | 6.3                                      | 4.1                                    | 5.6                  | 8                 | 2.9                                      | 4.4                                    | 11                   | 5                 |
| 24   | 13                                       | 19                                     | 8.5                  | 5                 | 7.9                                      | 12                                     | 9.0                  | 4                 | 6.1                                      | 4.0                                    | 5.3                  | 9                 | 2.9                                      | 4.4                                    | 10.0                 | 5                 |
| 25   | 12                                       | 19                                     | 8.6                  | 5                 | 8.0                                      | 12                                     | 8.5                  | 4                 | 5.9                                      | 3.8                                    | 5.0                  | 12                | 2.9                                      | 4.4                                    | 8.9                  | 6                 |
| 26   | 12                                       | 19                                     | 8.5                  | 5                 | 7.5                                      | 11                                     | 8.5                  | 4                 | 5.7                                      | 3.7                                    | 4.8                  | 15                | 2.9                                      | 4.4                                    | 7.4                  | 6                 |
| 27   | 13                                       | 19                                     | 9.0                  | 5                 | 4.2                                      | 6.5                                    | 9.5                  | 4                 | 5.5                                      | 3.6                                    | 4.5                  | 14                | 2.9                                      | 4.4                                    | 7.3                  | 8                 |
| 28   | 13                                       | 21                                     | 9.0                  | 7                 | 4.4                                      | 6.7                                    | 9.5                  | 4                 | 5.2                                      | 3.4                                    | 5.0                  | 13                | 2.9                                      | 4.4                                    | 7.5                  | 13                |
| 29   | 3.1                                      | 4.7                                    | 8.5                  | 12                | 3.7                                      | 5.6                                    | 9.0                  | 4                 | 5.0                                      | 3.3                                    | 5.5                  | 12                | 2.9                                      | 4.4                                    | 7.3                  | 12                |
| 30   | 2.7                                      | 4.1                                    | 8.5                  | 11                | 3.4                                      | 5.1                                    | 9.0                  | 11                | 4.8                                      | 3.2                                    | 5.2                  | 11                | 2.9                                      | 4.4                                    | 7.4                  | 11                |
| 31   | 2.4                                      | 3.6                                    | 8.5                  | 10                | 3.4                                      | 5.2                                    | 9.0                  | 10                | 4.6                                      | 3.0                                    | 5.0                  | 10                | 0.43                                     | 0.66                                   | 7.1                  | 10                |
| 32   | 1.6                                      | 2.5                                    | 6.7                  | 9                 | 2.4                                      | 3.7                                    | 9.0                  | 9                 | 4.4                                      | 2.9                                    | 4.7                  | 9                 | 0.43                                     | 0.66                                   | 5.5                  | 9                 |
| 33   | 1.1                                      | 1.7                                    | 5.1                  | 8                 | 2.9                                      | 4.5                                    | 10                   | 8                 | 4.2                                      | 2.8                                    | 3.0                  | 8                 | 0.43                                     | 0.66                                   | 4.3                  | 8                 |
| 34   | 0.73                                     | 1.1                                    | 3.8                  | 7                 | 0.58                                     | 0.89                                   | 10                   | 7                 | 4.0                                      | 2.6                                    | 2.5                  | 7                 | 0.43                                     | 0.66                                   | 3.2                  | 7                 |
| 35   | 0.47                                     | 0.72                                   | 2.7                  | 6                 | 0.0                                      | 0.0                                    | 0.0                  | 6                 | 3.8                                      | 2.5                                    | 1.8                  | 6                 | 0.43                                     | 0.66                                   | 2.2                  | 6                 |
| 36   | 0.32                                     | 0.50                                   | 2.0                  | 5                 | 0.0                                      | 0.0                                    | 0.0                  | 5                 | 3.6                                      | 2.3                                    | 1.2                  | 5                 | 0.43                                     | 0.66                                   | 1.6                  | 5                 |
| 37   | 0.16                                     | 0.25                                   | 1.0                  | 4                 | 0.0                                      | 0.0                                    | 0.0                  | 4                 | 3.4                                      | 2.2                                    | 0.86                 | 4                 | 0.43                                     | 0.66                                   | 0.83                 | 4                 |
| 38   | 0.070                                    | 0.11                                   | 0.46                 | 3                 | 0.0                                      | 0.0                                    | 0.0                  | 3                 | 3.2                                      | 2.1                                    | 0.60                 | 3                 | 0.43                                     | 0.66                                   | 0.35                 | 3                 |
| 39   | 0.031                                    | 0.047                                  | 0.21                 | 2                 | 0.0                                      | 0.0                                    | 0.0                  | 2                 | 3.0                                      | 1.9                                    | 0.42                 | 2                 | 0.43                                     | 0.66                                   | 0.15                 | 2                 |
| 40   | 0.011                                    | 0.017                                  | 0.073                | 1                 | 0.0                                      | 0.0                                    | 0.0                  | 1                 | 2.7                                      | 1.8                                    | 0.29                 | 1                 | 0.43                                     | 0.66                                   | 0.054                | 1                 |

## 4.0 Results

Predicted solute release is tabulated in Attachment A for all alternatives evaluated. The solute release from the embankment is compared to the solute load from the ore moisture and underground sump reporting to the process circuit. These sources are described and quantified by Enchemica (2018a). The solute load computed for the ore moisture and underground sump are summarized in Table 3 for selected constituents. The loads assume average flows during full production and average concentrations for the full life of mine. The solute release rates are summarized in Table 4, which assume maximum annual solute load for the life of mine.

Table 2. Pyrite stoichiometry

| Pyrite           |          |
|------------------|----------|
| Ag               | 4.17E-07 |
| As               | 3.88E-05 |
| Ba               | 1.36E-03 |
| Cd               | 3.68E-06 |
| Co               | 1.80E-04 |
| Cu               | 1.91E-02 |
| Mn               | 7.23E-03 |
| Mo               | 1.77E-04 |
| Ni               | 3.04E-04 |
| Pb               | 1.85E-06 |
| Sb               | 1.72E-05 |
| Zn               | 1.67E-03 |
| Se               | 1.33E-04 |
| S                | 3.30E-02 |
| FeS <sub>2</sub> | 1.00E+00 |

For sulfate, copper, manganese, zinc, arsenic, and selenium, the solute release rates from sulfide oxidation in the embankment are less than 2% of the solute load from the ore moisture and underground sump. The iron release rates from sulfide oxidation in the embankment are up to 28% of the iron load from the ore moisture and underground sump. Iron is expected to readily precipitate as ferrihydrite (not simulated in these predictions) under circumneutral conditions in the tailings and the process circuit. A large amount of lime will be added during processing to maintain circuit pH in the 8 to 8.5 range, therefore, any acidity generated by the precipitation of iron and other metals is unlikely to affect circuit pH.

Table 3. Solute load from the ore moisture and underground sump

|                            | Units  | Flow    | Units          | SO <sub>4</sub> | Cu             | Fe             | Mn             | Zn             | As             | Se             |
|----------------------------|--------|---------|----------------|-----------------|----------------|----------------|----------------|----------------|----------------|----------------|
| <b>Ore Moisture</b>        | gpm    | 914     | mg/L           | 2.8E+03         | 4.6E+02        | 6.3E+01        | 6.0E+00        | 1.3E+01        | 3.5E-02        | 8.5E-01        |
|                            | L/year | 1.8E+09 | mg/year        | 5.1E+12         | 8.3E+11        | 1.1E+11        | 1.1E+10        | 2.3E+10        | 6.4E+07        | 1.5E+09        |
|                            |        |         | kg/year        | 5.1E+06         | 8.3E+05        | 1.1E+05        | 1.1E+04        | 2.3E+04        | 6.4E+01        | 1.5E+03        |
| <b>Sump</b>                | gpm    | 2247    | mg/L           | 9.8E+02         | 1.5E-02        | 2.7E-03        | 2.1E-06        | 2.2E-01        | 6.4E-03        | 4.2E-03        |
|                            | L/year | 4.5E+09 | mg/year        | 4.4E+12         | 6.9E+07        | 1.2E+07        | 9.2E+03        | 1.0E+09        | 2.9E+07        | 1.9E+07        |
|                            |        |         | kg/year        | 4.4E+06         | 6.9E+01        | 1.2E+01        | 9.2E-03        | 1.0E+03        | 2.9E+01        | 1.9E+01        |
| <b>Ore Moisture + Sump</b> |        |         | <b>kg/year</b> | <b>9.5E+06</b>  | <b>8.3E+05</b> | <b>1.1E+05</b> | <b>1.1E+04</b> | <b>2.4E+04</b> | <b>9.2E+01</b> | <b>1.6E+03</b> |

Table 4. Solute release from embankment sulfide oxidation during operations

|                                       |         | SO <sub>4</sub> | Cu      | Fe      | Mn      | Zn      | As      | Se      |
|---------------------------------------|---------|-----------------|---------|---------|---------|---------|---------|---------|
| <b>Ops, Alt 2</b>                     | kg/year | 9.7E+04         | 6.0E+02 | 2.8E+04 | 2.0E+02 | 5.4E+01 | 1.4E+00 | 5.2E+00 |
| <b>Percent of ore moisture + sump</b> | %       | 1.02%           | 0.07%   | 24.34%  | 1.82%   | 0.23%   | 1.56%   | 0.33%   |
| <b>Ops, Alt 3</b>                     | kg/year | 8.9E+04         | 5.5E+02 | 2.5E+04 | 1.8E+02 | 5.0E+01 | 1.3E+00 | 4.8E+00 |
| <b>Percent of ore moisture + sump</b> | %       | 0.94%           | 0.07%   | 22.31%  | 1.67%   | 0.21%   | 1.43%   | 0.31%   |
| <b>Ops, Alt 5</b>                     | kg/year | 1.1E+05         | 6.9E+02 | 3.2E+04 | 2.3E+02 | 6.2E+01 | 1.7E+00 | 6.0E+00 |
| <b>Percent of ore moisture + sump</b> | %       | 1.18%           | 0.08%   | 28.01%  | 2.09%   | 0.26%   | 1.80%   | 0.39%   |
| <b>Ops, Alt 6</b>                     | kg/year | 7.5E+04         | 4.7E+02 | 2.1E+04 | 1.5E+02 | 4.2E+01 | 1.1E+00 | 4.0E+00 |
| <b>Percent of ore moisture + sump</b> | %       | 0.79%           | 0.06%   | 18.79%  | 1.40%   | 0.17%   | 1.21%   | 0.26%   |

From this comparison it can be concluded that:

- solute release from sulfide oxidation in the active embankment areas is small compared to other solute loads to the process circuit and likely within the uncertainty of the process circuit chemistry predictions;
- loads would likely be attenuated, to some degree, by chemical precipitation and sorption processes within the circuit; and
- the process circuit flow and solute balance models (Enchemica 2018b-f) do not need to incorporate a source term representing sulfide oxidation in the active embankment areas; and
- the differences on a site-to-site basis for each of the release parameters is small and likely lies close to or within the uncertainty limits of the analyses. Therefore, distinctions between options are unlikely to be sensitive to this component of loading.

## 5.0 References

- Enchemica 2018ba. Block Cave Geochemical Model – 2018 Update on Calculation Approach and Results. Tech. Memo. to H. Gluski (Resolution) from T. Eary (Enchemica). June 26.
- Enchemica 2018b. Alternative 2 - Near West Modified Proposed Action: Prediction of Operational Tailings Circuit Solute Chemistry. Tech. Memo. to V. Peacey (Resolution) from T. Eary (Enchemica). July 17.
- Enchemica 2018c. Alternative 3 - Near West Modified Proposed Action – Thin Lift/PAG Cell: Prediction of Operational Tailings Circuit Solute Chemistry. Tech. Memo. to V. Peacey (Resolution) from T. Eary (Enchemica). July 17.
- Enchemica 2018d. Alternative 5 - Peg Leg: Prediction of Operational Tailings Circuit Solute Chemistry. Tech. Memo. to V. Peacey (Resolution) from T. Eary (Enchemica). July 17.
- Enchemica 2018e. Alternative 6 - Skunk Camp Optimized: Prediction of Operational Tailings Circuit Solute Chemistry. Tech. Memo. to V. Peacey (Resolution) from T. Eary (Enchemica), August 14.
- Enchemica 2018f. Common Inputs Common to All Operational Models of Tailings Circuit Solute Chemistry. Tech. Memo. to V. Peacey (Resolution) from T. Eary (Enchemica). July 18.
- Golder Associates Inc. 2018 EIS Design. Peg Leg Site Alternative 5. Submitted to: Resolution Copper Mining LLC. Document Ref. 1788500-1000-1600-16-R-0. 6 August.
- Klohn Crippen Berger Ltd. (KCB). 2016. Resolution Copper Project – Near West Tailings Storage Facility Closure Cover Study. Prepared for Resolution Copper Mining. March.
- Klohn Crippen Berger Ltd. (KCB). 2018a. Resolution Copper Project – Tailings Storage Facility DEIS Designs – Tailings Geotechnical Characterization. April.
- Klohn Crippen Berger Ltd. (KCB). 2018b. Resolution Copper Project – DEIS Design for Alternative 3A Near West Modified Proposed Action (Modified Centerline Embankment – “wet”), Rev. 0. June.
- Klohn Crippen Berger Ltd. (KCB). 2018c. Resolution Copper Project – DEIS Design for Alternative 3B Near West Modified Proposed Action (High-density Thickened NPGAG Scavenger and Segregated PAG Pyrite Cell), Rev. 0. June.
- Klohn Crippen Berger Ltd. (KCB). 2018d. Resolution Copper Project – DEIS Design for Alternative 8 Skunk Camp, Rev. 0. June.
- Rio Tinto Growth and Innovation 2018. Prediction of tailings seepage water chemistry influenced by tailings weathering processes. Tech. Memo. from M. Wickham, Principal

Geochemist, G&I to V. Peacey, Senior Manager – Permitting and Approvals, Resolution Copper. 23 August.

**ATTACHMENT A  
TABULATED RESULTS  
SOLUTE LOAD FOR ACTIVE EMBANKMENT AREAS**

## Solute load for active embankment areas

Alternative 2. All results are in units of kg/year

| Year | Ag      | As      | Ba     | Cd      | Co      | Cu    | Mn     | Mo      | Ni      | Pb      | Sb      | Sr     | Zn     | Se      | Fe     | S      |
|------|---------|---------|--------|---------|---------|-------|--------|---------|---------|---------|---------|--------|--------|---------|--------|--------|
| 1    | 0.00038 | 0.025   | 1.6    | 0.0035  | 0.090   | 10    | 3.4    | 0.14    | 0.15    | 0.0032  | 0.018   | 2.3    | 0.92   | 0.089   | 472    | 550    |
| 2    | 0.0010  | 0.066   | 4.2    | 0.0094  | 0.24    | 27    | 9.0    | 0.38    | 0.40    | 0.0087  | 0.047   | 6.1    | 2.5    | 0.24    | 1,265  | 1,474  |
| 3    | 0.0023  | 0.15    | 9.7    | 0.021   | 0.55    | 63    | 21     | 0.88    | 0.92    | 0.020   | 0.11    | 14     | 5.6    | 0.55    | 2,892  | 3,368  |
| 4    | 0.0061  | 0.39    | 25     | 0.056   | 1.4     | 164   | 54     | 2.3     | 2.4     | 0.052   | 0.28    | 36     | 15     | 1.4     | 7,552  | 8,798  |
| 5    | 0.012   | 0.80    | 51     | 0.11    | 2.9     | 332   | 109    | 4.7     | 4.9     | 0.10    | 0.57    | 73     | 30     | 2.9     | 15,285 | 17,806 |
| 6    | 0.014   | 0.93    | 60     | 0.13    | 3.4     | 389   | 127    | 5.4     | 5.7     | 0.12    | 0.67    | 86     | 35     | 3.4     | 17,895 | 20,846 |
| 7    | 0.018   | 1.2     | 74     | 0.16    | 4.2     | 483   | 158    | 6.8     | 7.1     | 0.15    | 0.83    | 107    | 43     | 4.2     | 22,229 | 25,895 |
| 8    | 0.020   | 1.3     | 85     | 0.19    | 4.8     | 553   | 181    | 7.7     | 8.1     | 0.17    | 0.95    | 122    | 50     | 4.8     | 25,431 | 29,625 |
| 9    | 0.018   | 1.2     | 74     | 0.16    | 4.2     | 480   | 157    | 6.7     | 7.1     | 0.15    | 0.83    | 106    | 43     | 4.2     | 22,103 | 25,748 |
| 10   | 0.014   | 0.90    | 58     | 0.13    | 3.3     | 378   | 124    | 5.3     | 5.6     | 0.12    | 0.65    | 83     | 34     | 3.3     | 17,389 | 20,257 |
| 11   | 0.021   | 1.4     | 87     | 0.19    | 5.0     | 568   | 186    | 8.0     | 8.3     | 0.18    | 0.98    | 125    | 51     | 4.9     | 26,127 | 30,436 |
| 12   | 0.021   | 1.4     | 88     | 0.19    | 5.0     | 572   | 187    | 8.0     | 8.4     | 0.18    | 0.99    | 126    | 51     | 5.0     | 26,342 | 30,686 |
| 13   | 0.020   | 1.3     | 81     | 0.18    | 4.6     | 528   | 173    | 7.4     | 7.8     | 0.17    | 0.91    | 117    | 47     | 4.6     | 24,309 | 28,319 |
| 14   | 0.018   | 1.2     | 75     | 0.17    | 4.3     | 490   | 160    | 6.9     | 7.2     | 0.15    | 0.84    | 108    | 44     | 4.3     | 22,559 | 26,280 |
| 15   | 0.017   | 1.1     | 69     | 0.15    | 3.9     | 448   | 147    | 6.3     | 6.6     | 0.14    | 0.77    | 99     | 40     | 3.9     | 20,608 | 24,007 |
| 16   | 0.022   | 1.4     | 92     | 0.20    | 5.2     | 598   | 196    | 8.4     | 8.8     | 0.19    | 1.0     | 132    | 54     | 5.2     | 27,530 | 32,071 |
| 17   | 0.022   | 1.4     | 93     | 0.21    | 5.3     | 603   | 197    | 8.4     | 8.9     | 0.19    | 1.0     | 133    | 54     | 5.2     | 27,741 | 32,316 |
| 18   | 0.022   | 1.4     | 92     | 0.20    | 5.2     | 598   | 196    | 8.4     | 8.8     | 0.19    | 1.0     | 132    | 54     | 5.2     | 27,510 | 32,047 |
| 19   | 0.022   | 1.4     | 91     | 0.20    | 5.2     | 592   | 194    | 8.3     | 8.7     | 0.19    | 1.0     | 131    | 53     | 5.1     | 27,238 | 31,731 |
| 20   | 0.022   | 1.4     | 91     | 0.20    | 5.2     | 589   | 193    | 8.2     | 8.7     | 0.19    | 1.0     | 130    | 53     | 5.1     | 27,104 | 31,574 |
| 21   | 0.022   | 1.4     | 91     | 0.20    | 5.2     | 590   | 193    | 8.3     | 8.7     | 0.19    | 1.0     | 130    | 53     | 5.1     | 27,147 | 31,625 |
| 22   | 0.021   | 1.3     | 87     | 0.19    | 4.9     | 563   | 184    | 7.9     | 8.3     | 0.18    | 0.97    | 124    | 51     | 4.9     | 25,903 | 30,175 |
| 23   | 0.020   | 1.3     | 83     | 0.18    | 4.7     | 536   | 176    | 7.5     | 7.9     | 0.17    | 0.92    | 118    | 48     | 4.7     | 24,680 | 28,751 |
| 24   | 0.019   | 1.2     | 78     | 0.17    | 4.4     | 507   | 166    | 7.1     | 7.5     | 0.16    | 0.87    | 112    | 46     | 4.4     | 23,339 | 27,188 |
| 25   | 0.018   | 1.1     | 73     | 0.16    | 4.2     | 474   | 155    | 6.6     | 7.0     | 0.15    | 0.82    | 105    | 43     | 4.1     | 21,835 | 25,436 |
| 26   | 0.022   | 1.4     | 91     | 0.20    | 5.2     | 591   | 193    | 8.3     | 8.7     | 0.19    | 1.0     | 130    | 53     | 5.1     | 27,176 | 31,659 |
| 27   | 0.022   | 1.4     | 91     | 0.20    | 5.2     | 589   | 193    | 8.3     | 8.7     | 0.19    | 1.0     | 130    | 53     | 5.1     | 27,116 | 31,588 |
| 28   | 0.021   | 1.3     | 86     | 0.19    | 4.9     | 560   | 183    | 7.8     | 8.2     | 0.18    | 0.96    | 124    | 50     | 4.9     | 25,777 | 30,028 |
| 29   | 0.017   | 1.1     | 70     | 0.15    | 4.0     | 454   | 149    | 6.4     | 6.7     | 0.14    | 0.78    | 100    | 41     | 3.9     | 20,883 | 24,328 |
| 30   | 0.013   | 0.84    | 54     | 0.12    | 3.1     | 349   | 114    | 4.9     | 5.1     | 0.11    | 0.60    | 77     | 31     | 3.0     | 16,049 | 18,697 |
| 31   | 0.0090  | 0.58    | 38     | 0.083   | 2.1     | 244   | 80     | 3.4     | 3.6     | 0.077   | 0.42    | 54     | 22     | 2.1     | 11,219 | 13,069 |
| 32   | 0.0050  | 0.32    | 21     | 0.046   | 1.2     | 134   | 44     | 1.9     | 2.0     | 0.042   | 0.23    | 30     | 12     | 1.2     | 6,158  | 7,174  |
| 33   | 0.0052  | 0.34    | 22     | 0.048   | 1.2     | 140   | 46     | 2.0     | 2.1     | 0.044   | 0.24    | 31     | 13     | 1.2     | 6,453  | 7,518  |
| 34   | 0.0054  | 0.35    | 22     | 0.049   | 1.3     | 145   | 48     | 2.0     | 2.1     | 0.046   | 0.25    | 32     | 13     | 1.3     | 6,680  | 7,782  |
| 35   | 0.0022  | 0.14    | 9.0    | 0.020   | 0.51    | 58    | 19     | 0.82    | 0.86    | 0.018   | 0.10    | 13     | 5.2    | 0.51    | 2,682  | 3,125  |
| 36   | 0.0023  | 0.15    | 9.4    | 0.021   | 0.54    | 61    | 20     | 0.86    | 0.90    | 0.019   | 0.11    | 14     | 5.5    | 0.53    | 2,823  | 3,289  |
| 37   | 0.0023  | 0.15    | 9.7    | 0.022   | 0.55    | 63    | 21     | 0.89    | 0.93    | 0.020   | 0.11    | 14     | 5.7    | 0.55    | 2,911  | 3,391  |
| 38   | 0.0024  | 0.15    | 9.9    | 0.022   | 0.56    | 64    | 21     | 0.90    | 0.95    | 0.020   | 0.11    | 14     | 5.8    | 0.56    | 2,962  | 3,450  |
| 39   | 0.0024  | 0.16    | 10     | 0.022   | 0.57    | 65    | 21     | 0.91    | 0.96    | 0.021   | 0.11    | 14     | 5.9    | 0.57    | 2,995  | 3,489  |
| 40   | 0.0024  | 0.16    | 10     | 0.022   | 0.57    | 66    | 21     | 0.92    | 0.96    | 0.021   | 0.11    | 14     | 5.9    | 0.57    | 3,019  | 3,517  |
| 41   | 1.1E-06 | 7.0E-05 | 0.0045 | 1.0E-05 | 0.00026 | 0.029 | 0.0096 | 0.00041 | 0.00043 | 9.3E-06 | 5.0E-05 | 0.0065 | 0.0026 | 0.00025 | 1.3    | 1.6    |



## Solute load for active embankment areas

Alternative 5. All results are in units of kg/year

| Year | Ag     | As   | Ba  | Cd    | Co   | Cu  | Mn  | Mo   | Ni   | Pb    | Sb    | Sr  | Zn  | Se   | Fe     | S      |
|------|--------|------|-----|-------|------|-----|-----|------|------|-------|-------|-----|-----|------|--------|--------|
| 1    | 0.0    | 0.0  | 0.0 | 0.0   | 0.0  | 0.0 | 0.0 | 0.0  | 0.0  | 0.0   | 0.0   | 0.0 | 0.0 | 0.0  | 0.0    | 0.0    |
| 2    | 0.0    | 0.0  | 0.0 | 0.0   | 0.0  | 0.0 | 0.0 | 0.0  | 0.0  | 0.0   | 0.0   | 0.0 | 0.0 | 0.0  | 0.0    | 0.0    |
| 3    | 0.026  | 1.7  | 107 | 0.24  | 6.1  | 694 | 227 | 9.7  | 10   | 0.22  | 1.2   | 153 | 62  | 6.0  | 31,917 | 37,182 |
| 4    | 0.0033 | 0.21 | 14  | 0.031 | 0.79 | 90  | 29  | 1.3  | 1.3  | 0.028 | 0.15  | 20  | 8.1 | 0.78 | 4,126  | 4,806  |
| 5    | 0.0035 | 0.23 | 15  | 0.032 | 0.83 | 94  | 31  | 1.3  | 1.4  | 0.030 | 0.16  | 21  | 8.5 | 0.82 | 4,340  | 5,056  |
| 6    | 0.0019 | 0.12 | 8.0 | 0.018 | 0.45 | 52  | 17  | 0.73 | 0.76 | 0.016 | 0.089 | 11  | 4.7 | 0.45 | 2,385  | 2,778  |
| 7    | 0.0034 | 0.22 | 14  | 0.031 | 0.80 | 91  | 30  | 1.3  | 1.3  | 0.029 | 0.16  | 20  | 8.2 | 0.79 | 4,189  | 4,880  |
| 8    | 0.0027 | 0.18 | 11  | 0.025 | 0.64 | 73  | 24  | 1.0  | 1.1  | 0.023 | 0.13  | 16  | 6.6 | 0.64 | 3,372  | 3,928  |
| 9    | 0.0042 | 0.27 | 17  | 0.039 | 0.99 | 113 | 37  | 1.6  | 1.7  | 0.036 | 0.19  | 25  | 10  | 0.98 | 5,208  | 6,067  |
| 10   | 0.0041 | 0.27 | 17  | 0.038 | 0.98 | 111 | 36  | 1.6  | 1.6  | 0.035 | 0.19  | 25  | 10  | 0.97 | 5,130  | 5,976  |
| 11   | 0.0058 | 0.37 | 24  | 0.053 | 1.4  | 155 | 51  | 2.2  | 2.3  | 0.049 | 0.27  | 34  | 14  | 1.3  | 7,143  | 8,321  |
| 12   | 0.0063 | 0.41 | 26  | 0.058 | 1.5  | 171 | 56  | 2.4  | 2.5  | 0.054 | 0.29  | 38  | 15  | 1.5  | 7,850  | 9,145  |
| 13   | 0.0069 | 0.44 | 28  | 0.063 | 1.6  | 185 | 61  | 2.6  | 2.7  | 0.058 | 0.32  | 41  | 17  | 1.6  | 8,512  | 9,916  |
| 14   | 0.0087 | 0.56 | 36  | 0.080 | 2.0  | 234 | 76  | 3.3  | 3.4  | 0.074 | 0.40  | 52  | 21  | 2.0  | 10,747 | 12,519 |
| 15   | 0.0092 | 0.59 | 38  | 0.084 | 2.2  | 247 | 81  | 3.5  | 3.6  | 0.078 | 0.43  | 55  | 22  | 2.1  | 11,377 | 13,253 |
| 16   | 0.0095 | 0.61 | 39  | 0.087 | 2.2  | 257 | 84  | 3.6  | 3.8  | 0.081 | 0.44  | 57  | 23  | 2.2  | 11,809 | 13,757 |
| 17   | 0.0094 | 0.61 | 39  | 0.086 | 2.2  | 254 | 83  | 3.6  | 3.7  | 0.080 | 0.44  | 56  | 23  | 2.2  | 11,679 | 13,606 |
| 18   | 0.0091 | 0.59 | 38  | 0.084 | 2.2  | 247 | 81  | 3.5  | 3.6  | 0.078 | 0.42  | 54  | 22  | 2.1  | 11,347 | 13,219 |
| 19   | 0.011  | 0.69 | 44  | 0.098 | 2.5  | 288 | 94  | 4.0  | 4.2  | 0.091 | 0.50  | 63  | 26  | 2.5  | 13,237 | 15,420 |
| 20   | 0.010  | 0.67 | 43  | 0.095 | 2.4  | 279 | 91  | 3.9  | 4.1  | 0.088 | 0.48  | 62  | 25  | 2.4  | 12,861 | 14,983 |
| 21   | 0.0099 | 0.64 | 41  | 0.091 | 2.3  | 268 | 88  | 3.7  | 3.9  | 0.085 | 0.46  | 59  | 24  | 2.3  | 12,314 | 14,345 |
| 22   | 0.0094 | 0.60 | 39  | 0.086 | 2.2  | 253 | 83  | 3.5  | 3.7  | 0.080 | 0.44  | 56  | 23  | 2.2  | 11,624 | 13,541 |
| 23   | 0.011  | 0.69 | 45  | 0.099 | 2.5  | 290 | 95  | 4.1  | 4.3  | 0.092 | 0.50  | 64  | 26  | 2.5  | 13,325 | 15,522 |
| 24   | 0.010  | 0.66 | 42  | 0.094 | 2.4  | 275 | 90  | 3.8  | 4.0  | 0.087 | 0.47  | 61  | 25  | 2.4  | 12,643 | 14,728 |
| 25   | 0.0093 | 0.60 | 39  | 0.085 | 2.2  | 251 | 82  | 3.5  | 3.7  | 0.079 | 0.43  | 55  | 23  | 2.2  | 11,538 | 13,441 |
| 26   | 0.0100 | 0.64 | 41  | 0.091 | 2.4  | 269 | 88  | 3.8  | 3.9  | 0.085 | 0.46  | 59  | 24  | 2.3  | 12,357 | 14,395 |
| 27   | 0.0091 | 0.59 | 38  | 0.084 | 2.2  | 246 | 80  | 3.4  | 3.6  | 0.078 | 0.42  | 54  | 22  | 2.1  | 11,314 | 13,180 |
| 28   | 0.0083 | 0.54 | 35  | 0.076 | 2.0  | 225 | 73  | 3.1  | 3.3  | 0.071 | 0.39  | 50  | 20  | 1.9  | 10,332 | 12,036 |
| 29   | 0.0076 | 0.49 | 32  | 0.070 | 1.8  | 205 | 67  | 2.9  | 3.0  | 0.065 | 0.35  | 45  | 18  | 1.8  | 9,435  | 10,992 |
| 30   | 0.0070 | 0.45 | 29  | 0.064 | 1.6  | 188 | 61  | 2.6  | 2.8  | 0.059 | 0.32  | 41  | 17  | 1.6  | 8,636  | 10,060 |
| 31   | 0.0064 | 0.41 | 27  | 0.059 | 1.5  | 173 | 56  | 2.4  | 2.5  | 0.055 | 0.30  | 38  | 16  | 1.5  | 7,942  | 9,252  |
| 32   | 0.0073 | 0.47 | 30  | 0.067 | 1.7  | 196 | 64  | 2.7  | 2.9  | 0.062 | 0.34  | 43  | 18  | 1.7  | 9,010  | 10,496 |
| 33   | 0.0070 | 0.45 | 29  | 0.064 | 1.7  | 189 | 62  | 2.6  | 2.8  | 0.060 | 0.33  | 42  | 17  | 1.6  | 8,693  | 10,127 |
| 34   | 0.0080 | 0.52 | 33  | 0.074 | 1.9  | 216 | 71  | 3.0  | 3.2  | 0.068 | 0.37  | 48  | 19  | 1.9  | 9,937  | 11,577 |
| 35   | 0.0091 | 0.59 | 38  | 0.084 | 2.2  | 246 | 80  | 3.4  | 3.6  | 0.078 | 0.42  | 54  | 22  | 2.1  | 11,314 | 13,180 |
| 36   | 0.010  | 0.67 | 43  | 0.095 | 2.5  | 280 | 92  | 3.9  | 4.1  | 0.088 | 0.48  | 62  | 25  | 2.4  | 12,875 | 14,998 |
| 37   | 0.011  | 0.71 | 46  | 0.10  | 2.6  | 297 | 97  | 4.2  | 4.4  | 0.094 | 0.51  | 65  | 27  | 2.6  | 13,651 | 15,902 |
| 38   | 0.013  | 0.83 | 53  | 0.12  | 3.0  | 347 | 113 | 4.9  | 5.1  | 0.11  | 0.60  | 76  | 31  | 3.0  | 15,947 | 18,577 |
| 39   | 0.015  | 1.00 | 64  | 0.14  | 3.6  | 416 | 136 | 5.8  | 6.1  | 0.13  | 0.72  | 92  | 37  | 3.6  | 19,162 | 22,322 |
| 40   | 0.020  | 1.3  | 84  | 0.19  | 4.8  | 546 | 179 | 7.6  | 8.0  | 0.17  | 0.94  | 120 | 49  | 4.7  | 25,130 | 29,274 |
| 41   | 0.0044 | 0.29 | 18  | 0.041 | 1.0  | 120 | 39  | 1.7  | 1.8  | 0.038 | 0.21  | 26  | 11  | 1.0  | 5,505  | 6,413  |

## Solute load for active embankment areas

Alternative 6. All results are in units of kg/year

| Year | Ag      | As    | Ba  | Cd     | Co   | Cu  | Mn  | Mo   | Ni   | Pb     | Sb    | Sr  | Zn  | Se   | Fe     | S      |
|------|---------|-------|-----|--------|------|-----|-----|------|------|--------|-------|-----|-----|------|--------|--------|
| 1    | 0.0     | 0.0   | 0.0 | 0.0    | 0.0  | 0.0 | 0.0 | 0.0  | 0.0  | 0.0    | 0.0   | 0.0 | 0.0 | 0.0  | 0.0    | 0.0    |
| 2    | 0.0     | 0.0   | 0.0 | 0.0    | 0.0  | 0.0 | 0.0 | 0.0  | 0.0  | 0.0    | 0.0   | 0.0 | 0.0 | 0.0  | 0.0    | 0.0    |
| 3    | 0.0015  | 0.098 | 6.3 | 0.014  | 0.36 | 41  | 13  | 0.58 | 0.60 | 0.013  | 0.071 | 9.1 | 3.7 | 0.36 | 1,891  | 2,203  |
| 4    | 0.0030  | 0.20  | 13  | 0.028  | 0.72 | 82  | 27  | 1.2  | 1.2  | 0.026  | 0.14  | 18  | 7.4 | 0.71 | 3,782  | 4,406  |
| 5    | 0.0030  | 0.20  | 13  | 0.028  | 0.72 | 82  | 27  | 1.2  | 1.2  | 0.026  | 0.14  | 18  | 7.4 | 0.71 | 3,782  | 4,406  |
| 6    | 0.0044  | 0.28  | 18  | 0.040  | 1.0  | 118 | 39  | 1.7  | 1.7  | 0.037  | 0.20  | 26  | 11  | 1.0  | 5,424  | 6,319  |
| 7    | 0.0057  | 0.37  | 24  | 0.052  | 1.3  | 154 | 50  | 2.2  | 2.3  | 0.049  | 0.26  | 34  | 14  | 1.3  | 7,067  | 8,232  |
| 8    | 0.0047  | 0.31  | 20  | 0.044  | 1.1  | 128 | 42  | 1.8  | 1.9  | 0.040  | 0.22  | 28  | 12  | 1.1  | 5,889  | 6,860  |
| 9    | 0.0038  | 0.25  | 16  | 0.035  | 0.90 | 102 | 34  | 1.4  | 1.5  | 0.032  | 0.18  | 23  | 9.2 | 0.89 | 4,711  | 5,488  |
| 10   | 0.0057  | 0.37  | 24  | 0.052  | 1.3  | 154 | 50  | 2.2  | 2.3  | 0.049  | 0.26  | 34  | 14  | 1.3  | 7,067  | 8,232  |
| 11   | 0.0097  | 0.62  | 40  | 0.089  | 2.3  | 261 | 85  | 3.6  | 3.8  | 0.082  | 0.45  | 57  | 23  | 2.3  | 11,989 | 13,966 |
| 12   | 0.014   | 0.88  | 57  | 0.13   | 3.2  | 367 | 120 | 5.1  | 5.4  | 0.12   | 0.63  | 81  | 33  | 3.2  | 16,911 | 19,700 |
| 13   | 0.016   | 1.0   | 67  | 0.15   | 3.8  | 435 | 142 | 6.1  | 6.4  | 0.14   | 0.75  | 96  | 39  | 3.8  | 20,013 | 23,314 |
| 14   | 0.015   | 0.95  | 61  | 0.13   | 3.5  | 395 | 129 | 5.5  | 5.8  | 0.12   | 0.68  | 87  | 36  | 3.4  | 18,194 | 21,195 |
| 15   | 0.013   | 0.85  | 55  | 0.12   | 3.1  | 356 | 116 | 5.0  | 5.2  | 0.11   | 0.61  | 79  | 32  | 3.1  | 16,375 | 19,075 |
| 16   | 0.017   | 1.1   | 72  | 0.16   | 4.1  | 465 | 152 | 6.5  | 6.8  | 0.15   | 0.80  | 103 | 42  | 4.0  | 21,411 | 24,942 |
| 17   | 0.017   | 1.1   | 70  | 0.16   | 4.0  | 456 | 149 | 6.4  | 6.7  | 0.14   | 0.79  | 101 | 41  | 4.0  | 20,988 | 24,450 |
| 18   | 0.017   | 1.1   | 69  | 0.15   | 3.9  | 447 | 146 | 6.3  | 6.6  | 0.14   | 0.77  | 99  | 40  | 3.9  | 20,566 | 23,958 |
| 19   | 0.016   | 1.0   | 67  | 0.15   | 3.8  | 438 | 143 | 6.1  | 6.4  | 0.14   | 0.75  | 97  | 39  | 3.8  | 20,144 | 23,467 |
| 20   | 0.016   | 1.0   | 67  | 0.15   | 3.8  | 438 | 143 | 6.1  | 6.4  | 0.14   | 0.75  | 97  | 39  | 3.8  | 20,144 | 23,467 |
| 21   | 0.013   | 0.87  | 56  | 0.12   | 3.2  | 362 | 119 | 5.1  | 5.3  | 0.11   | 0.62  | 80  | 33  | 3.1  | 16,666 | 19,415 |
| 22   | 0.010   | 0.67  | 43  | 0.095  | 2.5  | 280 | 92  | 3.9  | 4.1  | 0.088  | 0.48  | 62  | 25  | 2.4  | 12,877 | 15,001 |
| 23   | 0.0073  | 0.47  | 30  | 0.067  | 1.7  | 197 | 65  | 2.8  | 2.9  | 0.062  | 0.34  | 44  | 18  | 1.7  | 9,088  | 10,587 |
| 24   | 0.0043  | 0.28  | 18  | 0.039  | 1.0  | 115 | 38  | 1.6  | 1.7  | 0.036  | 0.20  | 25  | 10  | 1.0  | 5,299  | 6,172  |
| 25   | 0.0039  | 0.25  | 16  | 0.035  | 0.91 | 104 | 34  | 1.5  | 1.5  | 0.033  | 0.18  | 23  | 9.3 | 0.90 | 4,779  | 5,567  |
| 26   | 0.0047  | 0.30  | 19  | 0.043  | 1.1  | 126 | 41  | 1.8  | 1.9  | 0.040  | 0.22  | 28  | 11  | 1.1  | 5,818  | 6,778  |
| 27   | 0.0043  | 0.28  | 18  | 0.040  | 1.0  | 116 | 38  | 1.6  | 1.7  | 0.037  | 0.20  | 26  | 10  | 1.0  | 5,350  | 6,233  |
| 28   | 0.0037  | 0.24  | 15  | 0.034  | 0.87 | 100 | 33  | 1.4  | 1.5  | 0.031  | 0.17  | 22  | 9.0 | 0.87 | 4,583  | 5,339  |
| 29   | 0.0031  | 0.20  | 13  | 0.029  | 0.73 | 84  | 27  | 1.2  | 1.2  | 0.026  | 0.14  | 18  | 7.5 | 0.73 | 3,856  | 4,492  |
| 30   | 0.0036  | 0.23  | 15  | 0.033  | 0.84 | 96  | 31  | 1.3  | 1.4  | 0.030  | 0.17  | 21  | 8.6 | 0.83 | 4,423  | 5,152  |
| 31   | 0.0028  | 0.18  | 12  | 0.026  | 0.66 | 76  | 25  | 1.1  | 1.1  | 0.024  | 0.13  | 17  | 6.8 | 0.66 | 3,477  | 4,051  |
| 32   | 0.0020  | 0.13  | 8.5 | 0.019  | 0.48 | 55  | 18  | 0.77 | 0.81 | 0.017  | 0.095 | 12  | 5.0 | 0.48 | 2,543  | 2,962  |
| 33   | 0.0021  | 0.14  | 8.9 | 0.020  | 0.51 | 58  | 19  | 0.81 | 0.85 | 0.018  | 0.100 | 13  | 5.2 | 0.50 | 2,660  | 3,098  |
| 34   | 0.0023  | 0.15  | 9.3 | 0.021  | 0.53 | 61  | 20  | 0.85 | 0.89 | 0.019  | 0.10  | 13  | 5.5 | 0.53 | 2,793  | 3,254  |
| 35   | 0.0017  | 0.11  | 7.3 | 0.016  | 0.41 | 47  | 15  | 0.66 | 0.69 | 0.015  | 0.081 | 10  | 4.2 | 0.41 | 2,170  | 2,528  |
| 36   | 0.0019  | 0.12  | 7.9 | 0.017  | 0.45 | 51  | 17  | 0.72 | 0.75 | 0.016  | 0.088 | 11  | 4.6 | 0.44 | 2,358  | 2,746  |
| 37   | 0.0021  | 0.13  | 8.7 | 0.019  | 0.49 | 56  | 18  | 0.79 | 0.83 | 0.018  | 0.097 | 12  | 5.1 | 0.49 | 2,592  | 3,019  |
| 38   | 0.0023  | 0.15  | 9.7 | 0.021  | 0.55 | 63  | 21  | 0.88 | 0.93 | 0.020  | 0.11  | 14  | 5.7 | 0.55 | 2,904  | 3,383  |
| 39   | 0.0027  | 0.18  | 11  | 0.025  | 0.64 | 73  | 24  | 1.0  | 1.1  | 0.023  | 0.13  | 16  | 6.6 | 0.64 | 3,372  | 3,928  |
| 40   | 0.0035  | 0.22  | 14  | 0.032  | 0.82 | 94  | 31  | 1.3  | 1.4  | 0.030  | 0.16  | 21  | 8.4 | 0.81 | 4,308  | 5,019  |
| 41   | 0.00075 | 0.049 | 3.1 | 0.0069 | 0.18 | 20  | 6.7 | 0.29 | 0.30 | 0.0064 | 0.035 | 4.5 | 1.8 | 0.18 | 936    | 1,091  |

**ATTACHMENT 2**  
**RTKC lysimeter chemistry summary**

## Technical memorandum

---

|                 |  |
|-----------------|--|
| From            | Matt Wickham, Principal Advisor, Geochemistry, Growth and Innovation                             |
| Department      | Growth & Innovation  |
| To              | File   |
| CC              | Brian Vinton (RTKC), Trevor Heaton (RTKC), Jacob Waples (Hydrogeologica), Victoria Peacey (RCML) |
| Reference       | RTKC tailings lysimeter summary  |
| Date            | 23 August 2018 (Final)   |
| Number of pages | 6  |

### 1.0 Introduction

This technical memorandum briefly summarizes background information and data collected for historical tailings lysimeters at the Rio Tinto Kennecott Copper (RTKC) south tailings impoundment near Magna, Utah. This summary was prepared to support tailings porewater predictions for the Resolution Copper draft environmental impact statement (DEIS), currently in preparation.

### 2.0 Background

The RTKC tailings impoundment includes both an historical South Impoundment, into which tailings were first deposited in 1915, and a North Impoundment that came into service in 1999. The impoundment is located northeast of the base of the northern flank of the Oquirrh Mountains and the southern shore of the Great Salt Lake. It is about 7 miles west of Salt Lake City, Utah, immediately north of the community of Magna. The tailings impoundments are bounded on the north by the Interstate 80 corridor, which separates the facility from the Great Salt Lake, by wetlands to the east and west, and by the Oquirrh Mountains and the town of Magna to the south. The tailings were generated by processing ore from the Bingham Canyon Mine, a porphyry copper deposit.

The climate at the tailings facilities is semi-arid. Mean annual precipitation at the Saltair weather station (the weather station closest to tailings impoundments) is 13.15 inches (1956-1991), which compares closely to the average annual precipitation at the Resolution Mine. Average pan evaporation at Saltair located near the impoundment is 70 inches, not including sublimation and evaporation during winter months, so this represents a minimum evaporation rate.

The South Impoundment, the relevant sub-domain for characterizing the tailings in this memorandum, was operational from the early 1900s to 2002, with reclamation occurring in stages beginning in 1998; the South Impoundment is currently inactive. The South Impoundment reaches a maximum elevation of approximately 4,445 feet above mean sea level (ft amsl), with tailings depths up to 245 feet thick, and occupies approximately 5,200 acres.

Various methods through time were used to construct the embankments around the South Impoundment and to deposit tailings in the impoundment. Embankment construction has been performed via centerline and upstream construction, including building starter dikes with on-site materials, mine rock fill materials, or trucked-in materials such as gravel (through the 1960s)

and construction of perimeter dikes of spigotted tailings (starting in 1971). Bulk whole tailings were deposited into the interior of the South Impoundment using a variety of methods, initially via several single point discharges along the southern limit of the impoundment. Beginning in 1956, tailings were deposited with peripheral spigot lines as well, to allow upstream construction methods. In 1988, the proportion of tailings distributed through the perimeter system increased to assist in controlling dust.

Final tailings deposition and reclamation of the South Impoundment began in 1998 and extended through 2002. The reclamation proceeded in a phased process across the South Impoundment. The South Impoundment was divided into five isolated reclamation areas by berms. Reclamation included deposition of a final lift layer of largely circumneutral whole tailings into each area as it was closed, facilitating direct revegetation on the final tailings surface.

### 3.0 Porewater sampling

Suction lysimeters were first installed in accessible areas of the South Impoundment in the mid-1990s<sup>1</sup> to support geochemical characterization of tailings. The characterization was used to guide design decisions for the North Impoundment design and to support permitting. Nested pressure-vacuum lysimeters (Soil Moisture Model 1920) were installed at depths of up to 20 feet below ground surface (ft bgs) and bedded in a fine silica sand in a manner consistent with manufacturer recommendations. Samples were collected from the lysimeters by RTKC or their contractors from 1994 to 2010 and analyzed for full chemistry. Nine of the lysimeters were included in the RTKC Ground Water Quality Discharge Permit UGW350011 until 2011, when they were removed from the permit conditions. A tabulated summary of the lysimeter details is provided in Table 1. The locations of the lysimeters are shown on Figure 1.

Samples were not filtered prior to analysis, however the maximum pore size for the ceramic lysimeter is 1.1 microns (field filtering commonly stipulates a 0.45 micron filter). Samples were analyzed for field pH, electrical conductivity, and temperature as well as alkalinity, aluminum, arsenic, calcium, chloride, copper, fluoride, iron, magnesium, manganese, potassium, selenium, sodium, sulfate, and zinc.

Groups of lysimeters were installed at several locations, with a different focus for each group. General background information and characteristics for each lysimeter group are provided below. Acid-base accounting (ABA) characteristics for the tailings, where known, are also summarized in Table 1. Sample results from nearby samples or general conditions are included where tailings samples were not collected and analyzed at the installed depths.

- **Step Back Area Lysimeters (TLL4100 through TLL4107):** Two groups of lysimeters were installed in the southeast portion of the South Impoundment where tailings were previously stepped back to unweight the southeast portion of the impoundment for geotechnical stability. Given their location and the step back, these lysimeters are installed in whole tailings that are older than those tailings deposited at the surface as a part of the reclamation activities which occurred in the late 1990s. The southern group (TLL4100 to TLL4103) were installed in tailings that were unsaturated from dewatering activities. The northern group (TLL4104 to TLL4107) were installed in, at that time, nearly saturated tailings. Lysimeters were completed at different depths in each the group, at depths of 4, 8, 12 and 20 ft bgs. The borehole logs note that the lysimeters are all completed in tailings that are gray to light gray and described as silty sand to sandy silt. Layering is also noted.

The step back lysimeters were monitored routinely between 1995 and 2010. Monitoring was initially monthly, with decreasing frequency to bi-annually and then annually with time. Monitoring of lysimeters TLL4100 to TLL4103 was included in the site Groundwater Quality Discharge permit, though samples were not always able to be obtained.

---

<sup>1</sup> Suction lysimeters were installed in the North Impoundment in 2016, and are not described here due to the short period of record.

- **Test Fill Lysimeters (TLL4110 through TLL4123):** In anticipation of construction of the North Impoundment with cyclone tailings, three test plots were constructed next to the South Impoundment with pilot plant cyclone tailings. The test plots were free standing, containing approximately 10 feet of cyclone tailings (including cover) and underlain by a drain (including a filter rock layer and drain rock layer) and liner (10 mil HDPE with a fine grit layer to protect the liner). Each of the three test plots had different cover configuration. Lysimeters were completed in each of the three test plots at depths ranging from 3 to 12 ft bgs. The borehole logs note that the lysimeters are all completed in tailings that are gray to light gray and described as silty sand to sandy silt. Geochemical characteristics (acid base accounting) were measured for some of the test fill materials and these data are presented in Table 1. The test fill lysimeters were routinely monitored between 1995 and 1997.
- **North embankment of the South Impoundment, TLL4124 to TLL4129:** The six lysimeters at this location were installed as three pairs, with a shallow and deep lysimeter in each pair. For TLL4128 and TLL4129, the lysimeters were completed at 2 and 5 feet ft bgs, respectively. Given their location on the embankment, it is assumed that these lysimeters are completed in embankment materials, which are expected to be relatively coarse to promote drainage for geotechnical stability.

The lysimeters were monitored routinely between 1995 and 2000. Monitoring was initially monthly, with decreasing frequency to bi-annually and then annually with time. Monitoring of lysimeters TLL4128 and TLL4129 was included in the site Groundwater Quality Discharge permit through 2010.

- **South Impoundment (TLL4130 to TLL4132):** These lysimeters were installed in a test plot that included biosolids amendment. The lysimeters were monitored briefly during 1996. No additional information is available about their installation or the tailings characteristics.
- **Southwest Embankment of the South Impoundment (TLL4133 to TLL4135):** Construction information, borehole logs, and tailings' geochemical characteristics are not available for the three lysimeters installed in the southwest embankment of the South Impoundment. It is assumed that these lysimeters were installed in a similar fashion (e.g., general construction and completion depths) as those for the step back area and test plot area based on the period of record monitored, and configuration and condition of the lysimeters.

The location of these lysimeters on the embankment implies that they are completed in relatively coarse materials typical of the embankments to promote drainage for geotechnical stability. Additionally, the pore water from these lysimeters is acidic. Combined with the location, this implies they are located in a well-drained environment in which oxygen can penetrate for sulfide oxidation and subsequent generation of acidic conditions. The pore water from TLL4134 and TLL4135 has a low pH and higher concentrations of sulfate and metals, implying that these lysimeters might be completed in a higher sulfide content material relative to that of TLL4133 or other lysimeters that do not indicate acidic conditions.

The southwest embankment lysimeters were monitored routinely between 1996 and 2010. Monitoring of lysimeters TLL4133 to TLL4135 was included in the site Groundwater Quality Discharge permit, though samples were not always able to be obtained due to unsaturated conditions.

- **South Impoundment (TLL4136 to TLL4138):** Other than location, no information is available about their installation or the tailings characteristics. Sampling was conducted from 1996 to 2001.

Table 1. Lysimeter summary

| Lysimeter Group | Lysimeter ID | Completion Depth (ft bgs) | Notes   | Historical Sampling Date Range | Sample count | Sample count for statistics | Average pH       | Lime <sup>2</sup> (% as CaCO <sub>3</sub> ) | ANP (kgCaCO <sub>3</sub> /t) | Total Sulfur (wt.%) | HNO <sub>3</sub> Extractable Sulfur (wt.%) | AGP (kgCaCO <sub>3</sub> /t) | NNP (kgCaCO <sub>3</sub> /t) | NPR         |     |  |
|-----------------|--------------|---------------------------|---|--------------------------------|--------------|-----------------------------|------------------|---|------------------------------|---------------------|--|------------------------------|------------------------------|-------------|-----|--|
| Step back area  | TL4100*      | 4.0                       | Site 1: South of well E3-B-501 in de-watered tailings area<br><br>Site 2: North of well E3-B-501 near step-back dike in nearly saturated tailings*<br><br>Site 3: cyclone overflow, un-vegetated, gravel cover, Depth to filter: 10.5', Depth to Drain a. 11.2'<br><br>Site 4: cyclone overflow, vegetated, no limestone, Depth to filter= 10.2', Depth to Drain = 10.8'<br><br>Plot 1: cyclone overflow lift, vegetated, limestone amended underflow layer, Depth to Filter= 9.6', Depth to Drain = 10.4'<br><br>Plot 2: cyclone overflow lift, vegetated, no limestone, Depth to filter= 10.2', Depth to Drain = 10.8'<br><br>Plot 3: cyclone overflow lift, vegetated, limestone amended underflow layer, Depth to Filter= 9.6', Depth to Drain = 10.4'<br><br>Plot 4: cyclone overflow lift, vegetated, no limestone amendment, Depth to Filter = 9.4', Depth to Drain = 9.9' | 8/29/1994                      | 31           | 31                          | 6.97             |   |                              |                     |  |                              |                              |             |     |  |
|                 | TL4101*      | 8.0                       |   | 10/14/1994                     | 40           | 40                          | 6.94             |   |                              |                     |  |                              |                              |             |     |  |
|                 | TL4102*      | 12.0                      |   | 8/29/1994                      | 37           | 37                          | 7.14             |   |                              |                     |  |                              |                              |             |     |  |
|                 | TL4103*      | 20.0                      |   | 8/29/1994                      | 39           | 39                          | 6.96             |   |                              |                     |  |                              |                              |             |     |  |
|                 | TL4104       | 4.0                       |   | 8/30/1994                      | 15           | 15                          | 7.02             | 2.3 +/- 0.95                                | 22.8                         | --                  | --   | 0.45 +/- 0.28                | 14.0 +/- 8.8                 | 8.7 +/- 8.1 | 1.6 |  |
|                 | TL4105       | 8.0                       |   | 8/30/1994                      | 15           | 15                          | 7.08             |   |                              |                     |  |                              |                              |             |     |  |
|                 | TL4106       | 12.0                      |   | 8/30/1994                      | 19           | 19                          | 7.27             |   |                              |                     |  |                              |                              |             |     |  |
|                 | TL4107       | 20.0                      |   | 8/30/1994                      | 20           | 20                          | 7.36             |   |                              |                     |  |                              |                              |             |     |  |
|                 | TL4110       | 3.0                       |   | 10/14/1994                     | 19           | 19                          | 7.41             |   |                              |                     |  |                              |                              |             |     |  |
|                 | TL4109       | 6.0                       |   | 11/10/1994                     | 18           | 18                          | 7.38             |   |                              |                     |  |                              |                              |             |     |  |
| Test Fill       | TL4108       | 8.0                       | 10/14/1994  | 19                             | 19           | 7.21                        | 1.3 +/- 0.72     | 12.8  | --                           | --                  | 0.38 +/- 0.14                              | 11.9 +/- 4.4                 | 0.93 +/- 7.31                | 1.1         |     |  |
|                 | TL4111       | 12.1                      | 11/10/1994  | 18                             | 18           | 7.48                        |                  |   |                              |                     |  |                              |                              |             |     |  |
|                 | TL4112       | 10.5                      | 11/10/1994  | 18                             | 18           | 7.41                        |                  |   |                              |                     |  |                              |                              |             |     |  |
|                 | TL4113       | 8.0                       | 11/10/1994  | 17                             | 17           | 7.13                        | 0.8              | 8.0   | 0.36                         | 0.24                | 0.24                                       | 7.5                          | 0.5                          | 1.1         |     |  |
|                 | TL4114       | 6.0                       | 11/10/1994  | 19                             | 19           | 7.18                        | 0.7              | 7.0   | 0.32                         | 0.21                | 0.21                                       | 6.6                          | 0.4                          | 1.1         |     |  |
|                 | TL4115       | 3.0                       | 11/10/1994  | 10                             | 9            | 6.76                        | --               | --  | --                           | --                  | --   | --                           | --                           | --          | --  |  |
|                 | TL4116       | 11.0                      | 11/10/1994  | 19                             | 18           | 6.99                        | --               | --  | --                           | --                  | --   | --                           | --                           | --          | --  |  |
|                 | TL4117       | 10.2                      | 11/10/1994  | 19                             | 19           | 7.24                        | 1.0              | 10.0  | 0.75                         | 0.57                | 0.57                                       | 17.8                         | -7.8                         | 0.56        |     |  |
|                 | TL4118       | 8.0                       | 11/10/1994  | 19                             | 19           | 7.51                        | 2.9              | 29.0  | 0.50                         | 0.36                | 0.36                                       | 11.3                         | 17.8                         | 2.6         |     |  |
|                 | TL4119       | 6.0                       | 11/10/1994  | 19                             | 19           | 7.42                        | 0.7              | 7.0   | 0.33                         | 0.25                | 0.25                                       | 7.8                          | -0.8                         | 0.90        |     |  |
|                 | TL4120       | 3.0                       | 1/19/1995   | 17                             | 17           | 7.26                        | 1.5              | 15.0  | 0.64                         | 0.49                | 0.49                                       | 15.3                         | -0.3                         | 1.0         |     |  |
|                 | TL4121       | 8.0                       | 11/10/1994  | 19                             | 19           | 6.93                        | --               | --  | --                           | --                  | --   | --                           | --                           | --          | --  |  |
|                 | TL4122       | 6.0                       | 11/10/1994  | 19                             | 19           | 7.07                        | 1.3              | 13.0  | 0.67                         | 0.52                | 0.52                                       | 16.3                         | -3.3                         | 0.80        |     |  |
| General         | TL4123       | 3.0                       | 11/10/1994  | 17                             | 17           | 7.33                        | 1.0              | 10.0  | 0.75                         | 0.75                | 0.57                                       | 17.8                         | -7.8                         | 0.56        |     |  |
|                 | TL4124       | 2.0                       | 1/17/1995   | 20                             | 0            | 3.94                        |                  |   |                              |                     |  |                              |                              |             |     |  |
|                 | TL4125       | 5.0                       | 1/17/1995   | 28                             | 28           | 6.67                        |                  |   |                              |                     |  |                              |                              |             |     |  |
|                 | TL4126       | 2.0                       | 5/25/2001   | 27                             | 27           | 7.40                        |                  |   |                              |                     |  |                              |                              |             |     |  |
|                 | TL4127       | 5.0                       | 5/25/2001   | 27                             | 27           | 7.00                        |                  |   |                              |                     |  |                              |                              |             |     |  |
|                 | TL4128*      | 2.0                       | 4/9/2009  | 41                             | 28           | 5.50                        | 2.3 +/- 0.9      | 18 +/- 9.8                                  | 1.3 +/- 0.68                 | 1.3 +/- 0.68        | 0.6 +/- 0.26                               | 19.2 +/- 8                   | -1.2 +/- 8                   | 1.0         |     |  |
|                 | TL4129*      | 5.0                       | 4/9/2009  | 34                             | 34           | 7.19                        |                  |   |                              |                     |  |                              |                              |             |     |  |
|                 | TL4130       | 3.0                       | 3/28/1996   | 3                              | 3            | 7.04                        |                  |   |                              |                     |  |                              |                              |             |     |  |
|                 | TL4131       | 5.0                       | 3/28/1996   | 4                              | 4            | 6.94                        |                  |   |                              |                     |  |                              |                              |             |     |  |
|                 | TL4132       | 7.0                       | 3/28/1996   | 4                              | 4            | 6.88                        |                  |   |                              |                     |  |                              |                              |             |     |  |
|                 | TL4133       | 3.0                       | 12/31/1996  | 16                             | 0            | 2.68                        |                  |   |                              |                     |  |                              |                              |             |     |  |
|                 | TL4134       | 5.0                       | 4/28/2004   | 16                             | 0            | 3.65                        | 1.7 <sup>1</sup> | 17.0  | 1.5                          | 1.5                 | 1.1  | 35.0                         | -18.0                        | 0.5         |     |  |
|                 | TL4135       | 7.0                       | 4/28/2004   | 18                             | 0            | 2.39                        |                  |   |                              |                     |  |                              |                              |             |     |  |
| TL4136          | 7.0          | 12/31/1996                | 4   | 0                              | 7.65         |                             |                  |   |                              |                     |  |                              |                              |             |     |  |
| TL4137          | 7.0          | 12/31/1996                | 7   | 0                              | 7.46         |                             |                  |   |                              |                     |  |                              |                              |             |     |  |
| TL4138          | 7.0          | 5/25/2001                 | 10  | 0                              | 7.52         |                             |                  |   |                              |                     |  |                              |                              |             |     |  |

Notes:  
 \* Monitored as part of the RTKC groundwater permit.  
 +/- indicates reported standard deviation for all test fill or step back samples  
 Based on tailings samples collected in 2012.  
 Grey text indicates lysimeter excluded from the statistical summary

2. The conventional nomenclature at the time of the historical analyses for units for percent neutralization was "Lime" percent as CaCO<sub>3</sub>.

## 4.0 Summary statistics

A statistical summary of the lysimeter chemistry is provided in Table 2. For use at RCML, only sample results with a field pH of 6 or higher were used. Data from lysimeters and TLL4133 to TLL4138 were excluded due to a lack of detail. A total of 761 sample records are available, 644 of which met the pH conditions and were used in the statistical analysis.

Table 2. Summary statistics, RTKC lysimeter chemistry

| Analyte  | Count | Min    | Quartile (%) |       |       | Max    |
|--|-------|--------|--------------|-------|-------|--------|
|  |       |        | 25%          | 50%   | 75%   |        |
| * Conductivity Field ( $\mu\text{S}/\text{cm}$ ) | 630   | 1,012  | 5,253        | 6,310 | 7,328 | 15,830 |
| * pH (Field)                                     | 638   | 6.0    | 7.0          | 7.2   | 7.4   | 9.2    |
| * Temperature (Field)                            | 638   | 2.0    | 10           | 14    | 19    | 29     |
| Alkalinity (mg/L as $\text{CaCO}_3$ )            | 511   | 2.5    | 96           | 200   | 261   | 942    |
| Aluminum (mg/L)                                  | 622   | 0.0050 | 0.10         | 0.27  | 0.60  | 716    |
| Arsenic (mg/L)                                   | 641   | 0.001  | 0.0080       | 0.016 | 0.027 | 0.23   |
| Calcium (mg/L)                                   | 635   | 1.0    | 526          | 634   | 743   | 1,330  |
| Chloride (mg/L)                                  | 580   | 5      | 320          | 1,070 | 1,353 | 2,830  |
| Copper (mg/L)                                    | 649   | 0.0010 | 0.020        | 0.080 | 0.20  | 837    |
| Fluoride (mg/L)                                  | 556   | 0.70   | 1.8          | 2.5   | 3.3   | 26     |
| Iron (mg/L)                                      | 654   | <0.01  | 0.20         | 0.30  | 0.30  | 449    |
| Magnesium (mg/L)                                 | 635   | 1.0    | 140          | 175   | 218   | 2,557  |
| Manganese (mg/L)                                 | 85    | <0.01  | 0.044        | 0.19  | 0.72  | 28     |
| Potassium (mg/L)                                 | 635   | 0.50   | 78           | 93    | 113   | 264    |
| Selenium (mg/L)                                  | 649   | 0.0015 | 0.009        | 0.018 | 0.040 | 0.28   |
| Sodium (mg/L)                                    | 635   | 1.0    | 584          | 784   | 1,033 | 3,250  |
| Sulfate (mg/L)                                   | 585   | 179    | 2,180        | 2,490 | 3,010 | 12,700 |
| Zinc (mg/L)                                      | 635   | <0.01  | 0.050        | 0.097 | 0.18  | 17     |

Notes:

\*Indicates field measurements

On-half the detection limit used for non-detect values for statistics

Non-detect minimums noted by "<" detection limit



FIGURE 1. LYSIMETER LOCATIONS  
SOUTH TAILINGS IMPOUNDMENT  
RIO TINTO KENNECOTT COPPER  
MAGNA, UTAH  
23 AUGUST 2018

**ATTACHMENT 3**

**Tabulated results, mixed seepage chemistry and solute loads**

Excel spreadsheet with results for Alternatives 2 through 6

MIM exchange factor  $1 \times 10^{-11} \text{ s}^{-1}$ .

Worksheet suffix **C** is concentrations

Worksheet suffix **M** is solute load

Filename: SOx Summary, 1E-11.xlsx  
(provided with document transmittal)

Excel spreadsheet with results for Alternatives 2 through 6

MIM exchange factor  $1 \times 10^{-12} \text{ s}^{-1}$ .

Worksheet suffix **C** is concentrations

Worksheet suffix **M** is solute load

Filename: SOx Summary, 1E-12.xlsx  
(provided with document transmittal)

August 25, 2018

Ms. Mary Rasmussen  
US Forest Service  
Supervisor's Office  
2324 East McDowell Road  
Phoenix, AZ 85006-2496

**Subject:** Response to Analysis Data Request #1 – Request for Tailings Seepage – Item #2 -  
Tailings Oxidation Potential of the Embankment

Dear Ms. Rasmussen,

To complete the response to item #2 from your March 8, 2018 letter, the following document is enclosed:

**2. Tailings Solute Modeling:** It is our understanding that the water balance and geochemical modeling for tailings solute is being updated, specific to each alternative tailings storage facility, and including specific analysis of oxidation potential of the embankment. There is an expectation that modeling would cover both operational and post-closure time frames.

**RCM Response:** As requested, please see the attached technical memorandum titled “*Prediction of tailings seepage water chemistry influenced by tailings weathering processes*” dated August 23, 2018:

Sincerely,



Vicky Peacey,

Senior Manager, Environment, Permitting and Approvals; Resolution Copper Company, as  
Manager of Resolution Copper Mining, LLC

Cc: Ms. Mary Morissette; Senior Environmental Specialist; Resolution Copper Company

Enclosure(s):

Technical Memorandum by Rio Tinto Growth & Innovation (2018), *Prediction of tailings seepage water chemistry influenced by tailings weathering processes.*